Article

Developmental Cell

Multi-layered Regulation of SPL15 and Cooperation with SOC1 Integrate Endogenous Flowering Pathways at the *Arabidopsis* Shoot Meristem

Graphical Abstract

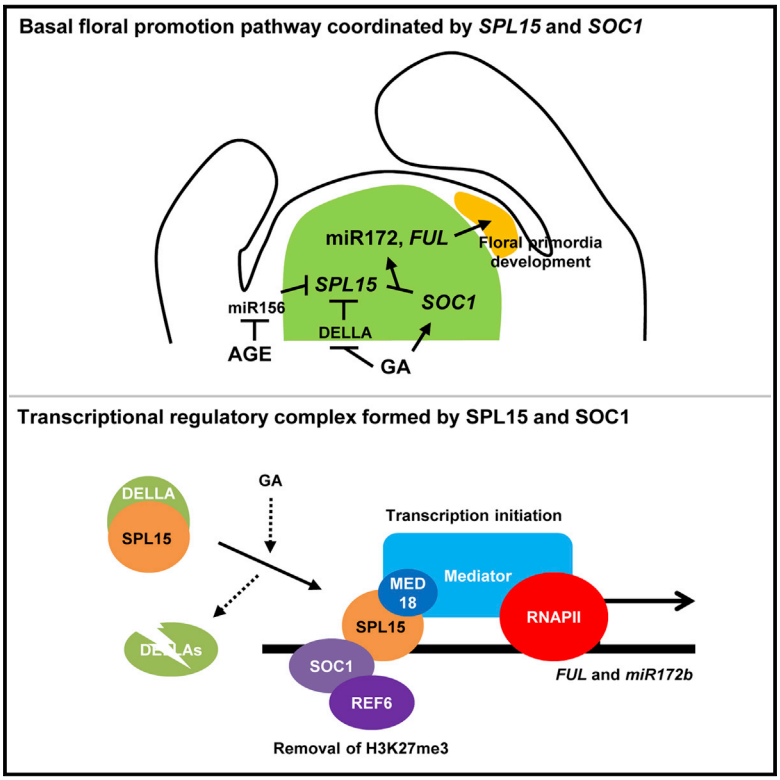

Highlights

- SPL15 coordinates floral initiation in *Arabidopsis* under non-inductive environments
- Flowering cues derived from plant age and phytohormone GA are integrated on SPL15
- SPL15 initiates transcription by recruiting MED18 and RNAPII in a GA-dependent manner
- SPL15 and SOC1 form a complex and cooperate to activate target gene transcription

Authors

Youbong Hyun, René Richter, Coral Vincent, Rafael Martinez-Gallegos, Aimone Porri, George Coupland

Correspondence

coupland@mpipz.mpg.de

In Brief

Hyun et al. demonstrate that the shoot meristem component SPL15, an *Arabidopsis* transcription factor, coordinates floral initiation under non-inductive environments by integrating cues derived from plant age and the phytohormone gibberellin. SPL15 recruits Mediator-RNAPII for transcriptional initiation of targets and cooperates with another transcription factor, SOC1, for transcriptional regulation.

Hyun et al., 2016, Developmental Cell *37*, 254–266
May 9, 2016
http://dx.doi.org/10.1016/j.devcel.2016.04.001

CellPress

CellPress

Developmental Cell
Article

Multi-layered Regulation of SPL15 and Cooperation with SOC1 Integrate Endogenous Flowering Pathways at the *Arabidopsis* Shoot Meristem

Youbong Hyun,[1,2] René Richter,[1,2] Coral Vincent,[1] Rafael Martinez-Gallegos,[1] Aimone Porri,[1] and George Coupland[1,*]
[1]Department of Plant Developmental Biology, Max Planck Institute for Plant Breeding Research, Carl-von-Linne Weg 10, 50829 Köln, Germany
[2]Co-first author
*Correspondence: coupland@mpipz.mpg.de
http://dx.doi.org/10.1016/j.devcel.2016.04.001

SUMMARY

Flowering is initiated in response to environmental and internal cues that are integrated at the shoot apical meristem (SAM). We show that *SPL15* coordinates the basal floral promotion pathways required for flowering of *Arabidopsis* in non-inductive environments. SPL15 directly activates transcription of the floral regulators *FUL* and *miR172b* in the SAM during floral induction, whereas its paralog *SPL9* is expressed later on the flanks of the SAM. The capacity of SPL15 to promote flowering is regulated by age through miR156, which targets *SPL15* mRNA, and gibberellin (GA), which releases SPL15 from DELLAs. Furthermore, SPL15 and the MADS-box protein SOC1 cooperate to promote transcription of their target genes. SPL15 recruits RNAPII and MED18, a Mediator complex component, in a GA-dependent manner, while SOC1 facilitates active chromatin formation with the histone demethylase REF6. Thus, we present a molecular basis for assimilation of flowering signals and transcriptional control at the SAM during flowering.

INTRODUCTION

The time at which plants initiate flower development is regulated by a complex combination of environmental and endogenous cues, generating plasticity in the timing of reproductive development and maximizing reproductive success (Andres and Coupland, 2012). The genetic and biochemical mechanisms by which these signals are integrated are poorly defined but are most thoroughly studied in *Arabidopsis thaliana*. Flowering of this species is regulated by day length, being promoted under long-day conditions (LDs; 16 hr light/8 hr dark) of summer and occurring much later under non-inductive short-day conditions (SDs; 8 hr light/16 hr dark). Genetic analyses demonstrated that the florigen protein FLOWERING LOCUS T (FT) promotes early flowering under LDs (Andres and Coupland, 2012), whereas the phytohormone gibberellin (GA) and reduction in the abundance of microRNA156 (miR156) induce flowering under SDs (Moon et al., 2003; Schwab et al., 2005; Wang et al., 2009; Wilson et al., 1992; Xu et al., 2016). The targets of miR156 are mRNAs encoding plant-specific transcription factors of the SQUAMOSA PROMOTER BINDING PROTEIN LIKE (SPL) family (Rhoades et al., 2002). Among 16 *SPL* genes in *A. thaliana*, the mRNAs of ten are targeted by miR156 and overexpression of the miRNA from heterologous promoters causes a complex pleiotropic phenotype (Schwab et al., 2005). The level of mature miR156 decreases as plants age (Bergonzi et al., 2013; Wang et al., 2011a; Wu and Poethig, 2006; Zhou et al., 2013), whereas constitutive overexpression of miR156 from a *35S::miR156* transgene extends the production of leaves with juvenile morphology in several plant species (Chuck et al., 2007; Wang et al., 2011a; Wu et al., 2009; Wu and Poethig, 2006). In *A. thaliana*, flowering of *35S::miR156* plants was also significantly delayed under SDs, while these plants exhibited only mild defects in flowering under LDs (Schwab et al., 2005; Wang et al., 2009). Furthermore, some members of the *SPL* family, notably SPL9 and SPL3, were described to bind directly to and regulate the expression of genes involved in floral development (Wang et al., 2009; Yamaguchi et al., 2009).

Flowering under SDs also requires GA, and *A. thaliana* mutants strongly impaired in GA biosynthesis, such as *ga1*, do not flower under these conditions (Wilson et al., 1992). Consistent with this conclusion, the levels of bioactive GA rapidly increase at the shoot apex shortly before floral initiation under SDs, while misexpression of GA catabolic enzymes or signaling components in specific tissues further showed that GA induces flowering via different floral pathway components in the leaves and SAM (Eriksson et al., 2006; Galvao et al., 2012; Porri et al., 2012). Notably, expressing the catabolic enzyme GIBBERELLIN 2 OXIDASE 7 (GA2ox7) from the *KNAT1* promoter at the shoot apex resulted in a delay of flowering in LDs and an extreme delay in SDs (Porri et al., 2012), but the molecular mechanism underlying this later flowering is not fully understood. GA signaling involves binding of the hormone to the GIBBERELLIN INSENSITIVE DWARF1 (GID1) receptors (Willige et al., 2007), which promote proteasome-mediated degradation of DELLA proteins (Fu et al., 2004; Murase et al., 2008; Silverstone et al., 2001). The misexpression of stabilized GA-insensitive variants of DELLA proteins at the shoot apex resulted in late flowering, indicating that GA signaling is required at the apex during floral induction (Galvao et al., 2012; Yu et al., 2012). Interestingly, *35S::miR156* plants showed a delayed flowering response to

exogenous GA under SDs, and a direct interaction between SPL9 and the DELLA protein REPRESSOR OF GA (RGA) has been described (Yamaguchi et al., 2014; Yu et al., 2012).

Integration of flowering signals in *A. thaliana* involves *SUPPRESSOR OF OVEREXPRESSION OF CONSTANS 1* (*SOC1*), which encodes a MADS-box transcription factor (Andres and Coupland, 2012; Lee and Lee, 2010). Loss-of-function *soc1* mutants are late flowering under LDs and SDs (Borner et al., 2000; Lee et al., 2000; Onouchi et al., 2000; Samach et al., 2000). The closely related MADS-box floral activator FRUITFULL (FUL) acts redundantly with SOC1, and *soc1 ful* double mutants show enhanced defects in floral initiation and maintenance of reproductive growth compared with the single mutants (Ferrandiz et al., 2000; Melzer et al., 2008; Torti et al., 2012). Several studies have described complex genetic interactions between *SOC1* and the GA- or miR156-derived floral pathways. For example, under SDs, overexpression of *SOC1* suppressed the flowering defects of *ga1* mutants (Moon et al., 2003). Additionally, *35S*::*miR156* showed reduced transcript levels of *SOC1* under the same conditions (Wang et al., 2009). *SOC1* is also involved in promoting the expression of the mRNAs of several *SPL* genes at the shoot apex during the floral transition under LDs (Torti et al., 2012), and *35S*::*miR156* compromised the accelerated flowering phenotypes of *35S*::*SOC1* in LDs (Jung et al., 2012).

Here we show that *SPL15*, a miR156-regulated member of the *SPL* family, is central to a basal floral promotion pathway. Regulation of SPL15 at the post-transcriptional and post-translational levels integrates the major cues of age and GA at the SAM to promote flowering under non-inductive conditions. Additionally, we demonstrate functional cooperation between SPL15 and SOC1 and define mechanisms by which they orchestrate transcriptional control of their direct target genes *FUL* and *miR172b*, which also encode floral regulators.

RESULTS

SPL15 Acts at the SAM and Has a Major Role in the Promotion of Flowering under Non-inductive Conditions

SPL15 and *SPL9* are closely related members of the group of miR156-targeted *SPLs* in *A. thaliana*. Previously, the flowering times of *spl9*, *spl15*, and *spl9 spl15* double mutants were reported under LDs, and *spl9 spl15* was shown to exhibit a mild delay in flowering (Schwarz et al., 2008). However, the roles of *SPL9* and *SPL15* have not been thoroughly examined under SDs, although *35S*::*miR156* transgenic plants showed a more significant delay in flowering under these conditions (Schwab et al., 2005; Wang et al., 2009). Flowering time of *spl15* mutants was therefore assessed under SDs, and a severe delay in flowering was observed, similar in severity to that of *spl9 spl15* (Figure 1A and Table S1). By contrast, *spl9* mutants flowered at almost the same time as Col under these conditions (Figure 1A and Table S1).

To further characterize the molecular effect of *SPL15* in flowering under SDs, we examined the transcripts of several floral regulator genes by qRT-PCR analyses using RNA extracted from plant apices. These analyses demonstrated that transcript levels of floral activators *FUL* and *miR172b*, a precursor of miR172 that targets *AP2*-like floral repressor genes (Aukerman and Sakai, 2003; Mathieu et al., 2009), were reduced in *spl15* mutants (Figure 1B). Whether *FUL* and *miR172b* are direct targets of SPL15 was examined by chromatin immunoprecipitation (ChIP) using an antibody raised against endogenous SPL15 (Figure S1A). Specific enrichment of fragments derived from the non-transcribed regions of both genes was detected by qPCR (Figures 1C and S1B). Interestingly, these genes were previously described as direct downstream targets of SPL9 (Wang et al., 2009; Wu et al., 2009).

Neither *spl9* nor *spl15* single mutants showed strong defects in flowering under LDs (Table S1) (Schwarz et al., 2008). In seedlings, no reduction of *FT* mRNA was detected in *spl9 spl15* double mutants (Figure S1C), suggesting that these SPL transcription factors do not act in leaves to promote flowering under LDs. By contrast, additive effects of *spl9* and *spl15* were detected in the transcriptional activation of *FUL* and *miR172b* also in LDs (Figure S1D), but *spl9 spl15* double mutants exhibited only a short delay in flowering and induction of the floral identity gene *LEAFY* (*LFY*) under these conditions (Table S1 and Figure S1D).

To understand the functional differences between *SPL15* and *SPL9* in promoting flowering under SDs, we compared the expression patterns of both genes at the SAM by in situ hybridization before and after the floral transition. Notably, the two genes exhibited distinct spatiotemporal patterns of mRNA accumulation (Figure 1D). *SPL15* mRNA was broadly detected in the SAM, and was present before as well as after the floral transition (Figure 1D). By contrast, *SPL9* mRNA was hardly detected at the SAM before floral induction (4w SD in Figure 1D), but became visible on the flanks of the SAM upon floral transition (6w SD in Figure 1D). The expression pattern of *SPL15* mRNA was also examined during transfer of plants from SD to LD to determine whether the limited role of *SPL15* in flowering under LDs is caused by differences in mRNA accumulation at the SAM (Figure S1E). This analysis revealed that the meristem-specific accumulation of *SPL15* mRNA is independent of day length. Consistent with this conclusion, the pattern of *SPL15* mRNA was not significantly affected in *ft tsf*, *soc1 ful*, *svp ft tsf*, and *svp soc1 ful* mutants that are impaired in the flowering response to LD in the SAM (Figure S1F) (Schmid et al., 2003; Torti et al., 2012).

Their spatial and temporal expression patterns suggested that during floral transition, *SPL9* and *SPL15* have their major functions in different tissues at distinct developmental times. To further test this possibility, we tested the accumulation of *FUL* mRNA and mature miR172 by in situ hybridization in the *spl* mutants through a time course under SDs (Figure 2). In wild-type plants, the levels of *FUL* mRNA and miR172 were strongly increased at the SAM during the floral transition (Figure 2). The spatial patterns in which *FUL* and miR172 were induced largely overlapped with the expression of *SPL15*, and the analysis of *spl15* mutants demonstrated that their accumulation strongly depended on the function of *SPL15*. In *spl9* mutants only a slight delay in *FUL* and miR172 induction was detected, and the apical sections showed that Col and *spl9* underwent the floral transition at similar times (Figure 2).

Overall, these results demonstrate crucial and previously unrecognized specific roles of *SPL15* in activating the transcription of key floral regulators at the SAM during floral transition under non-inductive conditions.

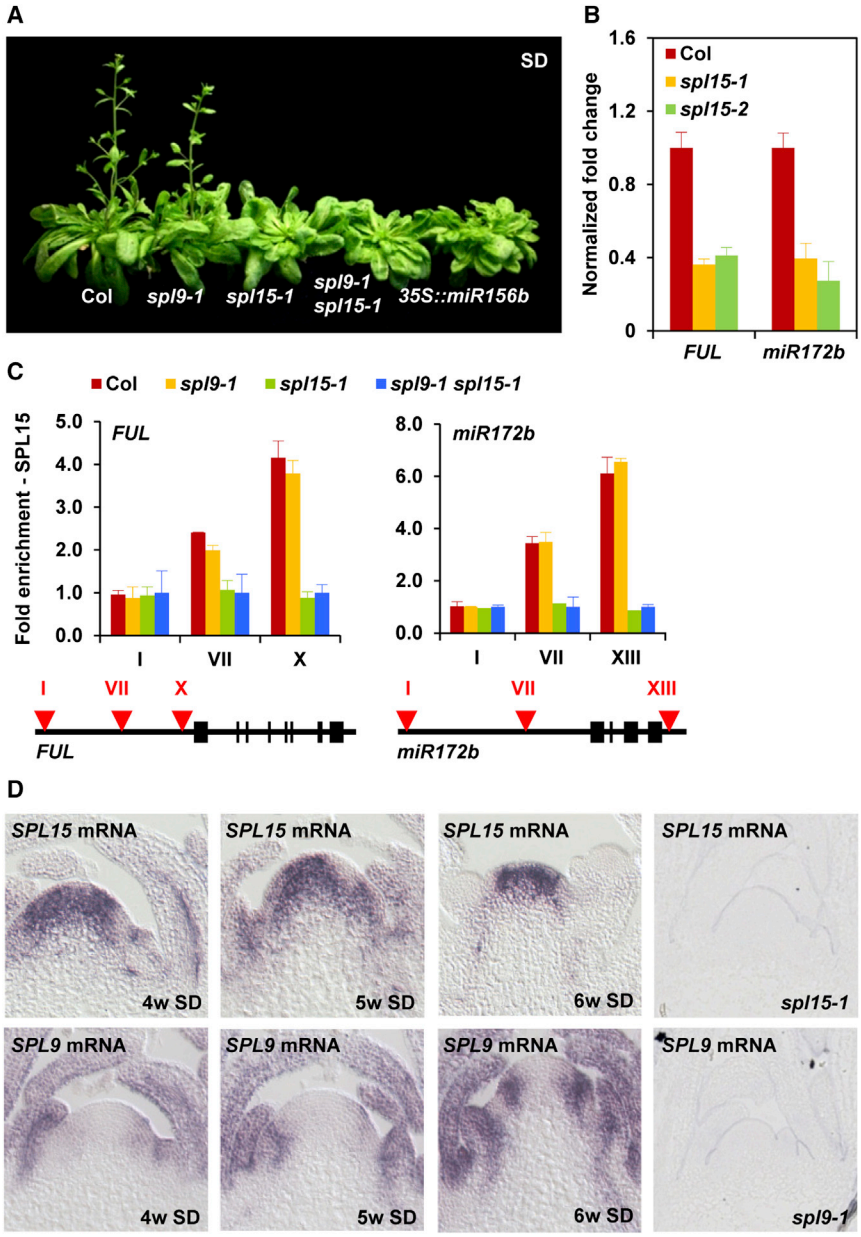

Figure 1. *SPL15* Promotes Flowering under Non-inductive Conditions

(A) Flowering phenotypes of *spl9*, *spl15*, *spl9 spl15*, and *35S*::*miR156b* in SD conditions.

(B) qRT-PCR analysis of *FUL* mRNA and *miR172b* precursor levels in shoot apices of 6-week-old plants grown under short-day conditions (SD). The transcript levels in Col are set to 1.0. Error bars indicate SD of three independent biological replicates.

(C) ChIP-qPCR analysis of SPL15 enrichment at *FUL* and *miR172b* genomic loci. Error bars indicate the SD of three biological replicates.

(D) In situ hybridization analysis of *SPL15* and *SPL9* mRNA accumulation in shoot apical meristems of Col under short-day (SD) conditions.

See also Figure S1.

SPL15 Integrates at the SAM Flowering Cues Derived from Age and GA

Flowering in SDs is repressed by miR156 overexpression, and the abundance of the miRNA falls progressively as plants become older (Schwab et al., 2005; Wang et al., 2009; Wu and Poethig, 2006). To test whether *SPL15* contributes to the age-related developmental phase transition, we constructed wild-type genomic *SPL15* clones and miR156-resistant mutant variants derived from them (Figure 3A). Additionally, in both clones the VENUS fluorescent protein was fused at the N terminus of SPL15 to allow visualization of protein accumulation (Figure 3A). Independent transgenic lines were identified that carried a single copy of the wild-type *SPL15*::*Venus9Ala*:*SPL15* (*V9A*:*SPL15*) transgene or the mutant variant *SPL15*::*Venus9Ala*:*rSPL15* (*V9A*:*rSPL15*).

Confocal microscopic analyses of representative lines revealed that the accumulation of SPL15 in the meristem increases with age and is regulated by miR156. In transgenic plants grown under SDs carrying the wild-type variant *V9A*:*SPL15*, fluorescence of V9A:SPL15 gradually increased as the plants became older (Figure 3B). By contrast, *V9A*:*rSPL15* plants showed relatively consistent levels of fluorescence (Figure 3B). Independent transgenic lines showed patterns of fluorescence similar to those of these representative lines (Figure S2A). Furthermore, the spatial pattern of protein accumulation was similar to that of *SPL15* mRNA, and strong acceleration of flowering was induced only by the miR156-resistant *V9A*:*rSPL15* transgene (Figure 3C). Under LDs, similar differences as under SDs in fusion protein accumulation and flowering time were observed between *V9A*:*rSPL15* and *V9A*:*SPL15* transgenic plants (Figures S2B and S2C).

SPL15 (Table S1) and GA (Wilson et al., 1992) are strongly involved in floral induction under SDs. Therefore, whether *SPL15* plays a role in GA-dependent floral regulation was tested by analyzing the flowering response of *spl15* mutants to exogenously applied GA. Remarkably, the acceleration of flowering by GA treatment of wild-type plants under SDs was significantly compromised in *spl15* but not in *spl9* mutants (Figure 3D and Table S1). Furthermore, SPL15 was found to interact with two different DELLA proteins, RGA and GAI, in the yeast two-hybrid system (Figure 3E). To test whether these DELLA proteins contribute to gene regulation by SPL15, we performed ChIP experiments with antibodies against RGA and showed enrichment patterns at similar regions of *FUL* and *miR172b* that were enriched by ChIP of SPL15 (Figure 3F). Interestingly, the enrichment of RGA at these positions was reduced in the *spl9*, *spl15*, and *spl9 spl15* mutants (Figures 3F and S3A) while RGA protein levels in these genotypes were not significantly changed (Figure S3B). Previous

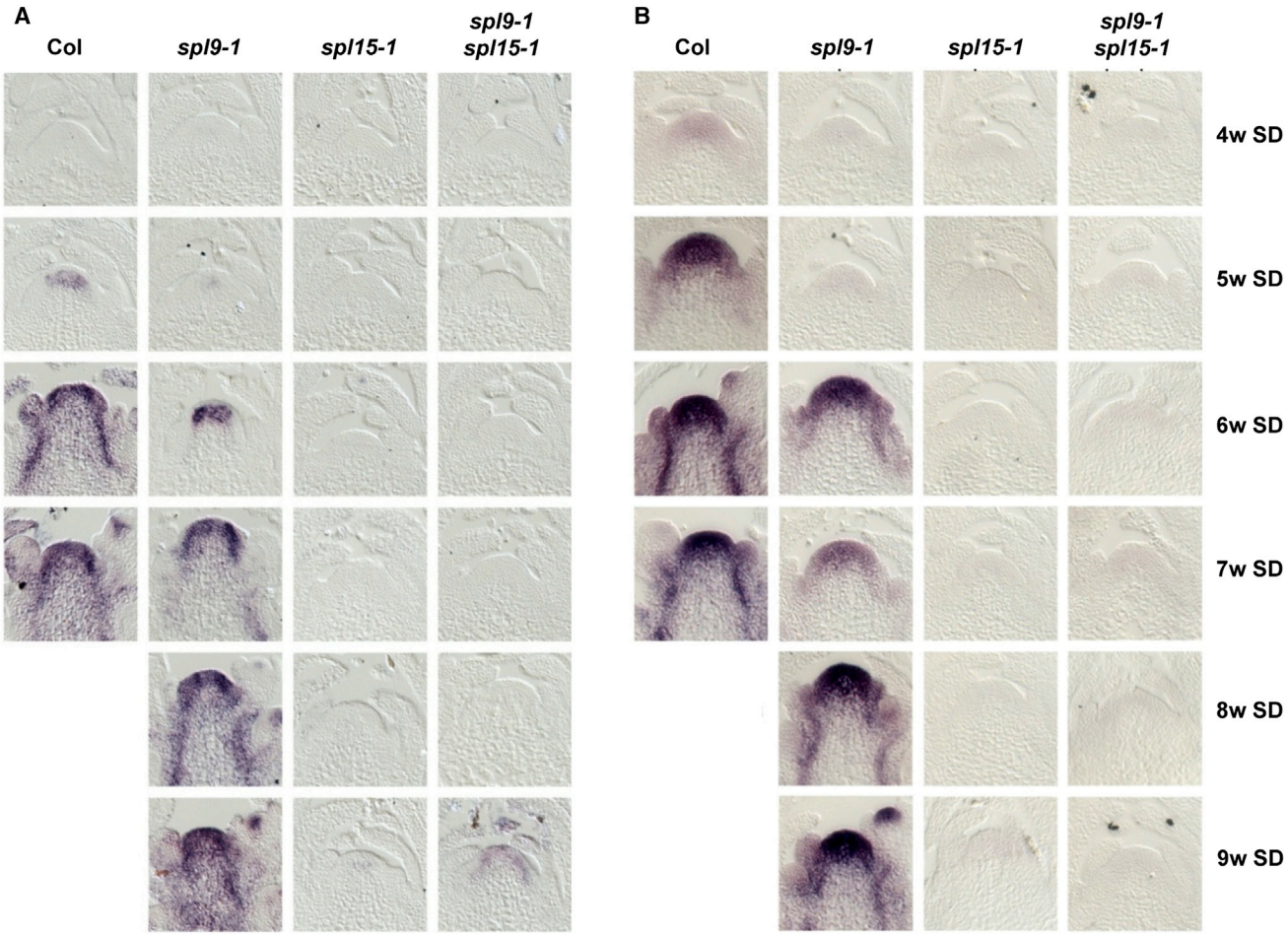

Figure 2. *SPL15* Mediates Accumulation of Floral Regulators at the SAM

In situ hybridization analysis of *FUL* mRNA (A) and mature miR172 (B) levels under short-day (SD) conditions. The genotypes analyzed are shown along with the number of weeks (w) after germination when they were harvested.

studies reported that RGA interacts with SPL9 (Yamaguchi et al., 2014; Yu et al., 2012), and the two proteins showed similar enrichment patterns in the genomic regions of *APETALA1* (*AP1*) (Yamaguchi et al., 2014). In our yeast two-hybrid assay, SPL9 also interacted with GAI, a homolog of RGA (Figure S3C). In addition, we observed that SPL9 associates with *FUL* and *miR172b* genomic regions in *SPL9*::*GFP:rSPL9* plants with enrichment profiles similar to those of SPL15 (Figure S3D). These results strongly support the idea that the DELLA proteins co-localize with both SPL9 and SPL15 on their target genes, but in different regions of the shoot apex based on the distinct spatiotemporal expression patterns of *SPL9* and *SPL15*.

Increased enrichment of RGA at loci bound by SPL15 was obtained in *ga1* mutants compared with wild-type (Figure 3F). Additionally, nuclear translocation of the RGA protein fused to the rat glucocorticoid receptor (GR) ligand binding domain resulted in reduced levels of *FUL* mRNA and *miR172b* precursor RNA after treatment with dexamethasone (DEX) in the presence of the protein synthesis inhibitor cycloheximide (CHX) (Figure 3G). These results suggest that increased DELLA levels block the ability of SPL15 to activate its target genes, and that this could therefore occur in GA-deficient conditions when DELLA levels rise and a stronger ChIP enrichment is detected with RGA at SPL15 targets. Consistent with this idea, the introduction of *KNAT1*::*GA2ox7* that catabolizes bioactive GA in the shoot apex strongly suppressed the promotion of flowering by *V9A*:*rSPL15*, as well as *FUL* and *miR172b* activation under SDs (Table S1 and Figure 3H).

Taken together, our results suggest that *SPL15* defines a basal floral promotion pathway active under non-inductive conditions and is a key component in the integration of age- and GA-derived flowering pathways at the SAM.

SPL15 Promotes Flowering in Cooperation with Floral Integrator SOC1

SOC1 was shown to interact genetically with miR156- and GA-dependent floral induction pathways under SDs (Moon et al., 2003; Wang et al., 2009). Therefore, the effect of SPL15 on *SOC1* mRNA levels was tested under these conditions. *SOC1* mRNA was detected broadly in the apex by in situ hybridization, but in contrast to *FUL* mRNA or miR172 the pattern of *SOC1* mRNA did not differ strongly between wild-type plants and

spl9, *spl15*, or *spl9 spl15* mutants (Figure S4). Together with the late-flowering phenotype of *spl15*, these results suggest that *SOC1* transcribed in *spl15* is not sufficient to induce flowering under SDs. Similarly, the early-flowering phenotype of *V9A:rSPL15* was strongly suppressed by loss-of-function alleles of *soc1* and *ful*, which encode related MADS-box transcription factors (Table S1). These results demonstrate that SPL15 and SOC1 are each required to promote flowering under SDs. In support of this idea, mutation of *SOC1* caused a strong reduction of *FUL* and *miR172b* transcript levels (Figures 4A and 4B) even though in *soc1* mutants SPL15 protein is present and can bind to its target regions in these genes (Figure S5A). Similarly, SOC1 bound to its target regions at *FUL* and *miR172b* independently of SPL15 (Figures 4C, S5B, and S5C). These results strongly suggest that SPL15 and SOC1, members of two different classes of DNA binding transcription factor, functionally cooperate to co-regulate a set of common target genes during the transition to flowering.

To address the biochemical functions of SPL15 and SOC1 in the transcriptional activation of their target genes, we monitored the enrichment of RNA polymerase II (RNAPII) along the transcribed regions of *FUL* and *miR172b*. Although the target genes showed a significant decrease in expression in both *spl9 spl15* and *soc1* mutants, the ChIP analysis of RNAPII revealed distinct profiles in the two mutants (Figures 4D and 4E). The enrichment of RNAPII observed in Col was absent in *spl9 spl15* throughout the transcribed regions of both target genes (Figure 4D). By contrast, in *soc1* mutants the loss of RNAPII enrichment was most apparent in regions of the gene body (Figure 4E), which has been described for transcriptionally inactive genes at which the RNAPII machinery is poised at the promoter area (Adelman and Lis, 2012). Taken together, our study describes functional cooperation between SPL15 and SOC1 in the regulation of flowering and target gene activation, but that the two different transcription factors play independent roles in the transcriptional activation process.

SPL15 and SOC1 Orchestrate Transcriptional Activation through Recruitment of Mediator Complex and Histone Demethylase REF6

Mediator (Med) complex in eukaryotes recruits the RNAPII machinery to genes upon interaction with specific transcription factors (Malik and Roeder, 2010). In *A. thaliana*, the Med complex is involved in diverse biological processes (Bonawitz et al., 2014; Hemsley et al., 2014). Notably, loss of function of MED18, a subunit of the Med complex, resulted in delayed flowering and reduced floral response to GA (Zheng et al., 2013). As *spl15* mutation caused a reduced flowering response to GA and failure to recruit RNAPII, we examined the functional relationship between SPL15 and MED18. Using yeast two-hybrid analysis, an interaction between SPL15 and MED18 was detected (Figure 5A). Moreover, V9A:SPL15 and MED18 proteins were co-immunoprecipitated in protein extracts from shoot apical tissues of *V9A:rSPL15* plants (Figures 5B and 5C), suggesting a direct involvement of SPL15 in the recruitment of the Med complex in planta. The co-immunoprecipitation (coIP) of V9A:SPL15 and MED18 was greatly reduced in *V9A:rSPL15 KNAT1::GA2ox7* plants whereas RGA showed higher levels of interaction with V9A:SPL15 in this genotype (Figure 5C). Furthermore, in yeast three-hybrid assays, the observed interaction between SPL15 and MED18 was strongly reduced in the presence of RGA (Figure 5D). ChIP-qPCR analysis revealed significant loss of the subunit at *FUL* and *miR172b* loci in *spl9 spl15* mutants (Figure 5E). Similarly, enrichment of MED18 at these loci was compromised in the *KNAT1::GA2ox7* backgrounds (Figure 5E). These results suggest that SPL15 initiates transcription of *FUL* and *miR172b* through recruitment of the Med complex and that this interaction is inhibited in GA-deficient conditions, probably by binding of DELLAs to SPL15.

SOC1 was also co-immunoprecipitated with V9A:SPL15 (Figure 5C), suggesting that it contributes to the same transcriptional complex. The observation that SOC1 and SPL15 bind distal and proximal to the transcriptional start site of *FUL*, respectively, suggested that formation of this complex might involve DNA looping as a critical determinant for *FUL* activation. Therefore, the chromosome conformation capture (3C) assay was employed (Figure 6A) (Hagege et al., 2007; Liu et al., 2014) to test for DNA looping involving the distally located enhancer CArG box predicted to bind SOC1 and the proximally located binding sites for SOC1 and SPL15 (Figure 4C). Taken together, the analyses suggested that the interaction between the distal enhancer and the proximally located CArG box occurred in a SOC1-dependent manner and that SPL9 and SPL15 stabilized the SOC1-induced DNA loop at the *FUL* locus (Figure 6A).

A previous study identified RELATIVE OF EARLY FLOWERING 6 (REF6) in the purified complex of MADS-box proteins functioning in floral organ development (Smaczniak et al., 2012). *REF6* encodes a JUMONJI C-domain histone demethylase that mediates active removal of the repressive H3K27me3 histone mark (Lu et al., 2011), and *ref6* mutants are late flowering (Noh et al., 2004). To address the role of SOC1 in transcriptional regulation, we tested for a physical interaction between SOC1 and REF6. In *REF6::REF6:HA ref6* transgenic plants, coIP between SOC1 and REF6:HA fusion proteins was detected (Figure 6B). Also, association of REF6:HA with the *FUL* and *miR172b* loci was tested in a ChIP assay, and similar genomic regions were found to be enriched as detected with SOC1 (Figures 6C and S6A).

In combination with the observed RNAPII ChIP patterns in *soc1* mutants (Figure 4E), these results suggest that SOC1 might generate an active chromatin state through the REF6-mediated removal of H3K27me3 repressive marks, thereby allowing RNAPII progression toward the coding region and efficient gene transcription. Consistent with this idea, increased levels of H3K27me3 histone marks were detected at *FUL* genomic regions in both *soc1* and *ref6* mutants with similar patterns in both genotypes (Figures 6D and 6E). Interestingly, after DEX-induced introduction of SOC1:GR proteins into the nucleus, DNA binding of SOC1 at the earliest time point tested preceded the reduction of H3K27me3 and transcriptional activation of *FUL* and *miR172b* (Figures S6B–S6F), further supporting the causal effects of SOC1 binding on active chromatin formation. Increased enrichment of H3K27me3 at *FUL* was detected also in *spl15* mutants (Figure 6F) while neither the interaction between SOC1 and REF6 nor REF6 recruitment were significantly changed in *spl9 spl15* mutants (Figures 6B and 6C), suggesting that SPL15 is required for removal of H3K27me3 after recruitment of SOC1-REF6 to the promoter, perhaps through stabilizing DNA looping (Figure 6A).

Taken together, our results suggest that SPL15 and SOC1 coordinate transcriptional activation processes of their target

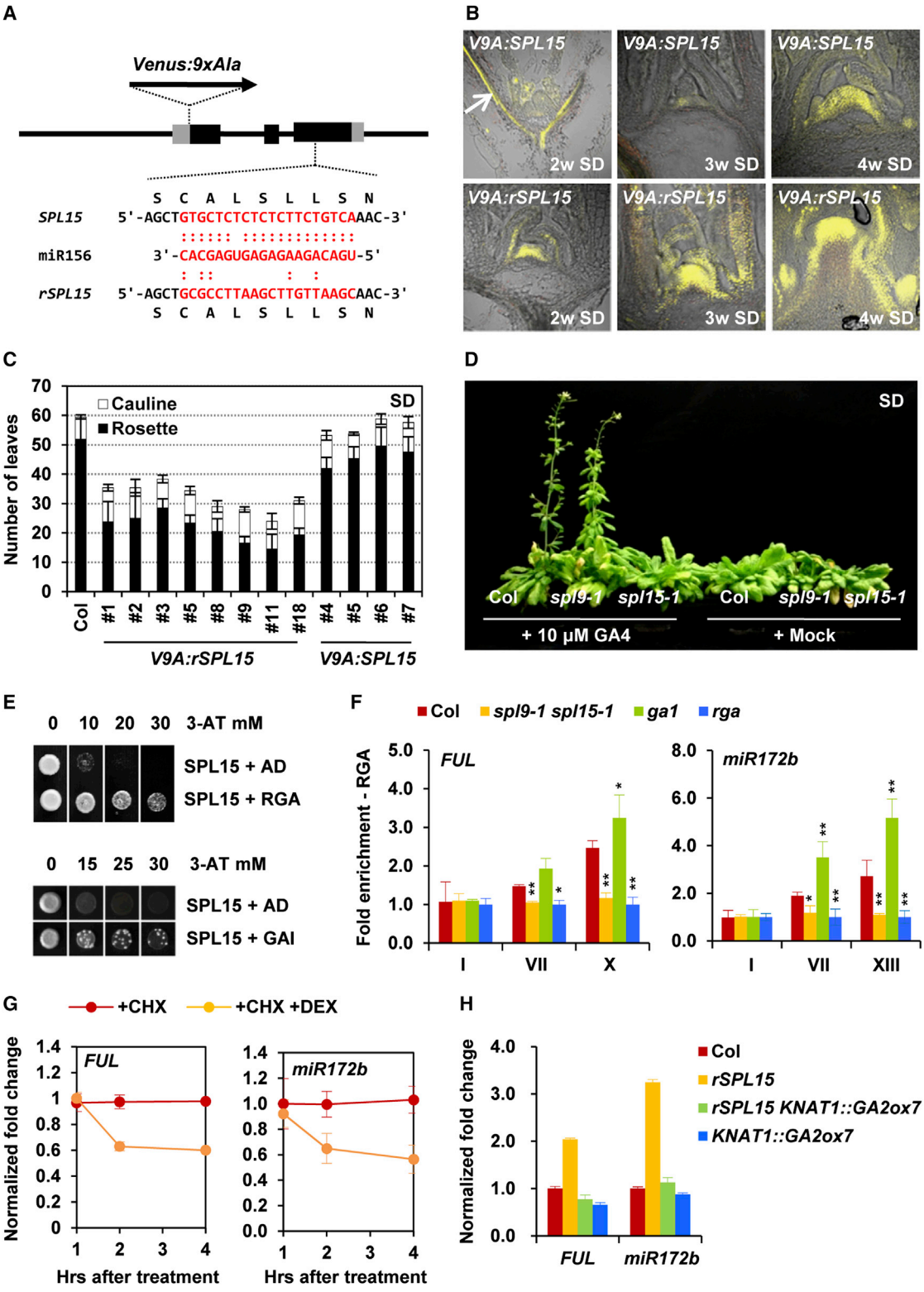

Figure 3. *SPL15* Integrates at the SAM Flowering Cues Derived from Age and GA

(A) Schematic structure of *V9A:SPL15* and *V9A:rSPL15* transgenes. Gray and black boxes represent UTR and exons in the transcribed region of *SPL15*, respectively. Target site of miR156 in *SPL15* and the incorporated mutation at the target site are shown with nucleotide sequences in red, and amino acid sequences encoded in the region are presented with single-letter amino acid codes.

(legend continued on next page)

genes *FUL* and *miR172b* through the recruitment of RNAPII and the establishment of an active chromatin state for floral induction.

DISCUSSION

The molecular basis of plasticity in the behavior of the SAM during floral induction is poorly understood. Here we show that SPL15, whose contribution to flowering has been little studied, plays a critical role in promoting the transition to flowering under non-inductive SDs through activation of target genes in cooperation with SOC1 (Figure 7A).

Specific Roles of *SPL15* in SDs in *A. thaliana* and Implications for Competence to Flower

Age-related flowering in *Arabidopsis* was previously proposed to involve miR156 regulation of genes that encode SPL transcription factors (Huijser and Schmid, 2011; Wang et al., 2009). However, precisely which members of the *SPL* family are involved and where they act has been difficult to discern because of assumed genetic redundancy between closely related members and lack of loss-of-function alleles for many *SPL* genes. Previous genome analysis indicated that *SPL9* and *SPL15* are located in distinct genomic blocks that arose in a progenitor of *A. thaliana* during a whole-genome duplication event called *At*α that is shared by all extant species of the Brassicaceae (Bowers et al., 2003). Despite the close evolutionary history of these genes, our analyses of loss-of-function mutations of *SPL15* and *SPL9* showed that *SPL15* has a strong effect on flowering in SDs downstream of GA that is clearly separable from its paralog *SPL9*. Whereas *SPL9* has been implicated in conferring floral primordium identity (Yamaguchi et al., 2014), our in situ hybridization, confocal microscopy, and analysis of target gene expression data demonstrate that *SPL15* acts earlier in the SAM to promote flowering downstream of miR156.

Under LDs, where the *spl15* phenotype is much weaker, the FT and TSF proteins produced in leaves move to the shoot apex and promote the floral transition (Andres and Coupland, 2012). FT interacts with another LD-specific floral regulator FD, which is expressed at the shoot apex (Abe et al., 2005; Wigge et al., 2005). Most LD-induced gene expression profiles in the SAM depend on the functions of *FT* and *TSF* (Schmid et al., 2003; Torti et al., 2012). We show that the accumulation of *SPL15* mRNA occurs independently of LD-derived flowering cues (Figures S1E and S1F). Additionally, even in LDs, *SPL15* increases the transcription of downstream targets *FUL* and *miR172b* (Figure S1D), although the late-flowering phenotype of *spl15* is weak under these conditions. Taken together, these results indicate that the floral promotion function of SPL15 in the meristem is less important under LDs than SDs, and that independent genetic networks are therefore employed to promote flowering in the meristem under LDs and SDs.

SPL15 is required for the timely accumulation of mature miR172 at the shoot apex under SDs (Figure 2). This miRNA targets a small class of *AP2*-like genes in *A. thaliana* (Aukerman and Sakai, 2003; Chen, 2004; Huijser and Schmid, 2011), and was previously shown to be rapidly activated in leaves by an inducible form of *SPL9* (Wu et al., 2009). Mutations in *AP2* and related *AP2*-like genes cause a strong acceleration of flowering in SDs (Mathieu et al., 2009; Yant et al., 2010). These results suggest that *SPL15* confers reproductive competence on the SAM at least in part by activation of miR172 expression, which in turn reduces the inhibition of flowering caused by *AP2*-like genes. Although the direct transcriptional regulation of the *miR172b* precursor by SPL15 was shown in our study, SPL15 might act either directly or indirectly on additional precursor loci, which would explain the dramatic reduction of miR172 detected in *spl15* mutant apices (Figure 2).

Roles of SPL15 in Transcriptional Activation

We show that SPL15 promotes transcription of downstream targets through the recruitment of MED18 and RNAPII (Figure 7B). SPL9 was previously found to directly activate transcription of *FUL* and *miR172b*, the same targets as SPL15 (Wang et al., 2009; Wu et al., 2009). Therefore, the additive effects observed in the *spl9 spl15* double mutant in qRT-PCR of target gene expression or ChIP-qPCR analyses of binding to target genes likely represent the combined effects of SPL9 and SPL15 acting in different tissues present in the samples. Under GA-deficient conditions, SPL15 showed reduced interaction with MED18 while stronger coIP of SPL15 and RGA was detected (Figure 5C). In yeast, the interaction between SPL15 and MED18 was also found to be compromised by the presence of RGA (Figure 5D). A similar biochemical relationship was recently reported among the key jasmonate (JA) signaling components JAZ, MYC, and MED25 (Zhang et al., 2015). JAZ9, a signaling repressor degraded by JA perception, showed competitive binding to MYC3 transcription factor with the Med complex component MED25. MYC3 was shown to undergo profound conformational changes if bound to JAZ9, thereby blocking the interaction between MYC3 and MED25. These observations suggest that a similar structural basis might exist for the GA-dependent relationship among SPL15, DELLA, and MED18.

(B) Confocal microscopic analysis of the fusion protein accumulation in wild-type *V9A:SPL15* and mutant variant *V9A:rSPL15* under short-day conditions (SD). Arrow indicates autofluorescence from tracheary elements in vasculature that fluoresces at wavelengths different from Venus fluorescent proteins (520 nm).
(C) Flowering times of *V9A:SPL15* and *V9A:rSPL15* transgenic plants grown under SD conditions. Numbers of leaves were measured in T3 homozygous populations of the independent transgenic lines. More than 20 plants of each single independent line were analyzed.
(D) Floral responses of *spl* mutants to exogenous GA treatment under short-day conditions (SD).
(E) Yeast two-hybrid analysis of the protein interaction of SPL15 with RGA and GAI.
(F) ChIP-qPCR analysis of RGA enrichment at *FUL* and *miR172b* genomic loci. Error bars indicate the SD of three biological replicates. Significance of differences from Col are shown by *p < 0.05, **p < 0.01 by Student's t test.
(G) qRT-PCR analysis of *FUL* and *miR172b* levels in *35S::RGA:GR rga rgl ga1* with DEX and CHX treatment. Transcript levels in +CHX samples at 1hr-after treatment are set to 1.0. Error bars indicate the SD of three independent biological replicates.
(H) qRT-PCR analysis of *FUL* mRNA and *miR172b* precursor levels in shoot apices of *V9A:rSPL15 KNAT1::GA2ox7* at 2 weeks after germination under short-day conditions. The transcript levels in Col are set to 1.0. Error bars indicate the SD of three independent biological replicates.
See also Figures S2 and S3.

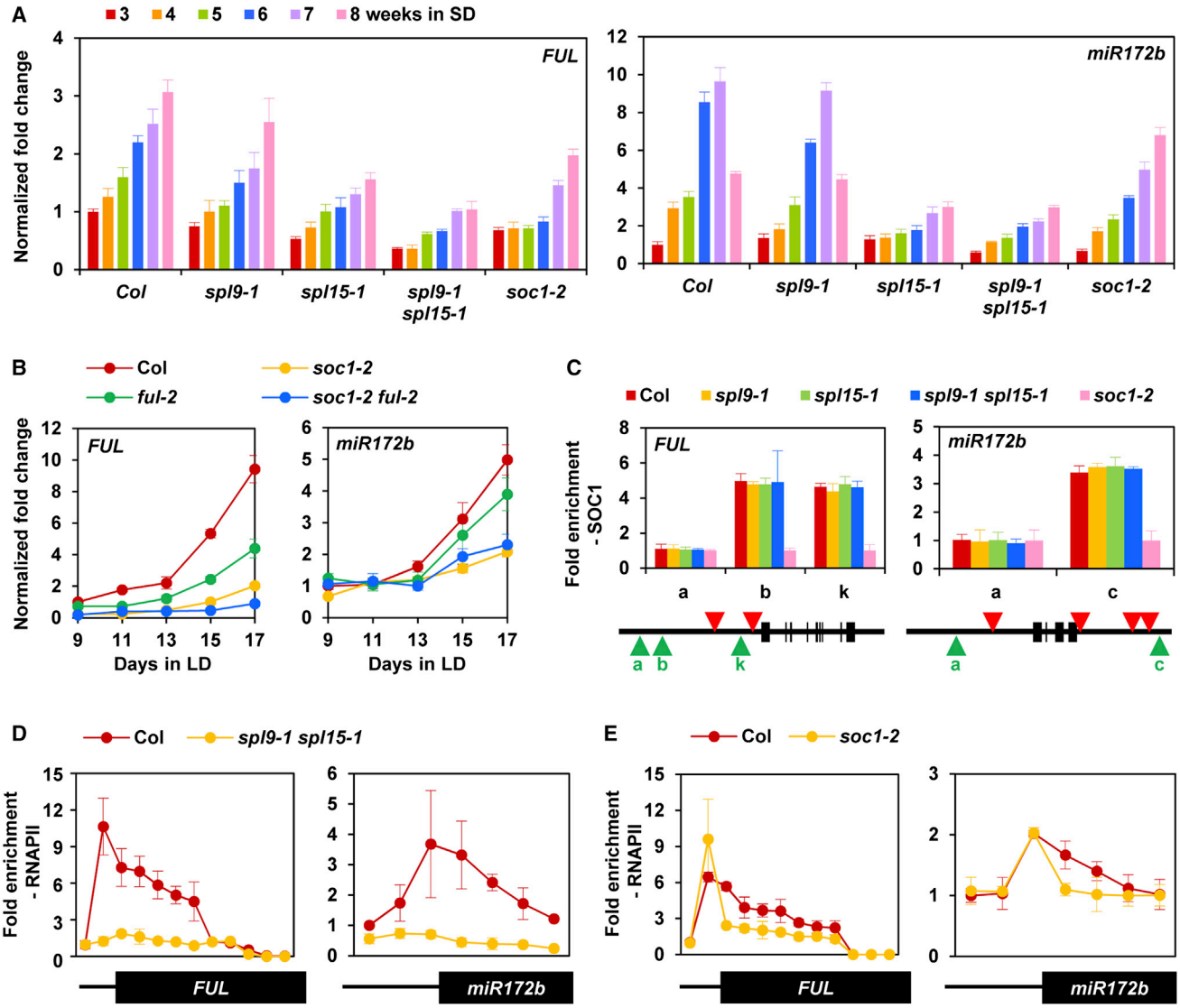

Figure 4. Functional Cooperation between SPL15 and SOC1

(A and B) qRT-PCR analysis of *FUL* and *miR172b* transcript levels in *spl* and *soc1* mutants under short-day conditions (A) and in *soc1*, *ful*, and *soc1 ful* mutants under long-day conditions (B). Transcript levels in Col plants grown for 3 weeks of short days and 9 long days are set to 1.0. Error bars indicate the SD of three independent biological replicates.

(C) ChIP-qPCR analysis of SOC1 enrichment at *FUL* and *miR172b* genomic loci. Positions of the analyzed amplicons and the SPL15-enriched regions are marked with green and red arrowheads, respectively.

(D and E) ChIP-qPCR analysis of RNAPII enrichment in the transcribed regions of *FUL* and *miR172b* in *spl9 spl15* (D) and *soc1* (E) mutants. The transcribed regions of the analyzed genes are marked with black boxes that match with positions of the analyzed amplicons.

Error bars indicate the SD of three independent biological replicates.

See also Figures S4 and S5.

Recently SPL9 was shown to activate transcription of the floral identity gene *AP1* after the initiation of flowering (Yamaguchi et al., 2014). Interestingly, in the later stages of floral induction we also observed strong accumulation of *SPL9* mRNA at the flanks of the SAM where *AP1* is initially induced (Figure 1D). Also, SPL9-DELLA complex was previously shown to activate transcription of *AP1* after the depletion of GA in the incipient floral primordium (Yamaguchi et al., 2014), whereas DELLA interaction represses the activity of SPL15. These observations suggest that the functions of the two related genes *SPL9* and *SPL15* diverged during evolution through the diversification of protein activity as well as differences in their transcriptional patterns. Alternatively, the biochemical function of SPL-DELLA complex might vary depending on the target loci to which they bind or the cell types in which they function.

Functional Cooperation between *SPL15* and *SOC1*

We demonstrated functional cooperation between two different types of DNA binding proteins, SPL15 and SOC1, on their direct target genes *FUL* and *miR172b* (Figure 7B). Genome-wide

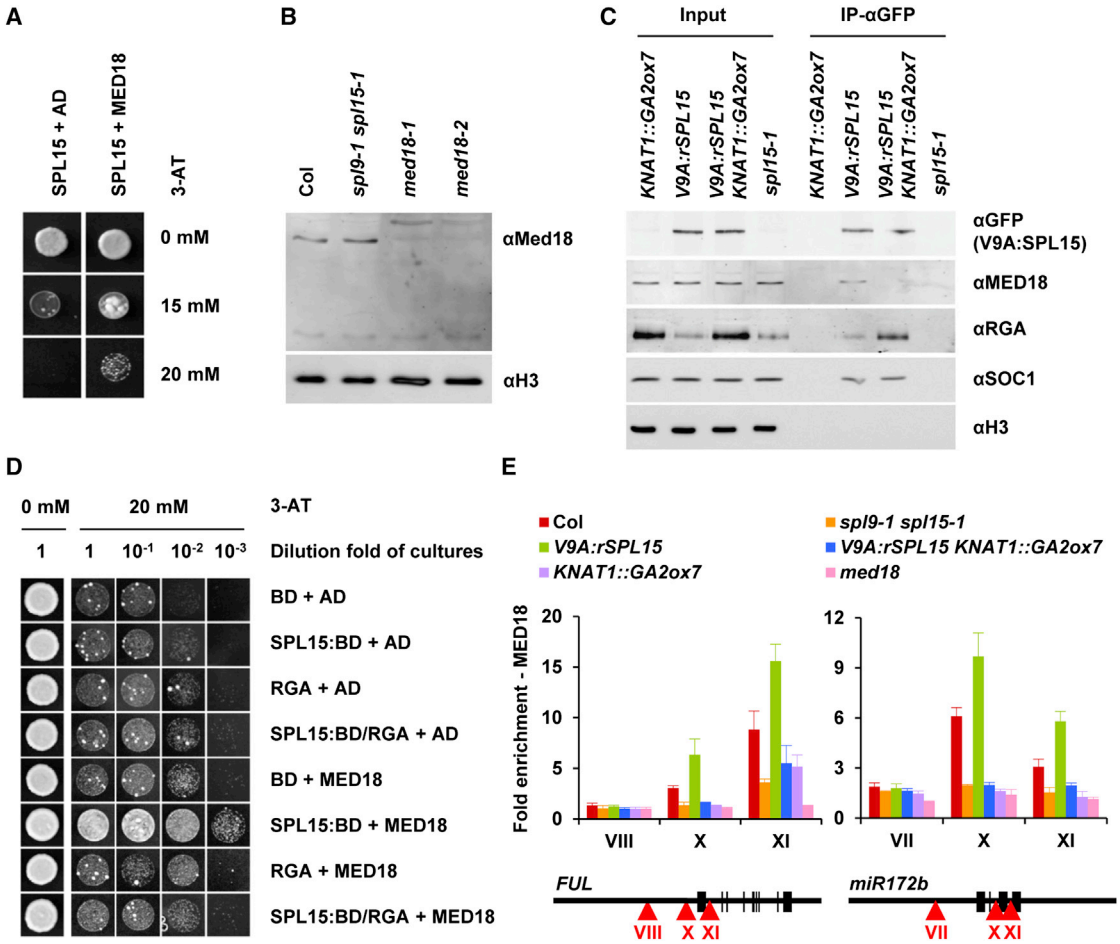

Figure 5. Roles of SPL15 in Med Complex Recruitment

(A) Yeast two-hybrid analysis of the protein interaction of SPL15 with MED18.

(B) Western blot analysis performed with antibodies for Med18.

(C) In vivo coIP analysis of the protein interaction among SPL15, MED18, RGA, and SOC1 in plants containing combinations of *V9A:rSPL15* and *KNAT1*::*GA2ox7* transgenes.

(D) Yeast three-hybrid analysis of the protein interaction of SPL15 with MED18 in the presence or absence of RGA.

(E) ChIP-qPCR analysis of MED18 enrichment at *FUL* and *miR172b* genomic loci. Positions of the analyzed amplicons correspond to those in Figure S1B.

profiles of SOC1 targets (Immink et al., 2012; Tao et al., 2012) did not identify *FUL* and *miR172b*. However, our experiments tested SOC1 binding at developmental time points different to those analyzed in the genome-wide studies. In addition, the binding to *FUL* and *miR172b* may not have been identified because the enrichment of SOC1 was below the stringency of target isolation in the genome-scale analyses. Interestingly, the genome-wide profiles of SOC1 targets revealed that the proteins directly repress many *AP2*-like genes (Immink et al., 2012; Tao et al., 2012). As *SPL15* and *SOC1* are involved in the accumulation of miR172 at the shoot apex and this reduces the expression of AP2-like proteins, these observations suggest that *SPL15* and *SOC1* regulate *AP2*-like genes both directly and indirectly during the transition to flowering.

In *spl15* mutants, SOC1-REF6 complex was detected at target loci (Figures 4C, 6B, and 6C) but the removal of H3K27me3 was significantly compromised (Figure 6F). A recent study in *Caenorhabditis elegans* reported that the pioneer transcription factor PHA-4 recruits RNAPII to condensed target genomic regions, and the RNAPII recruitment was shown to lead to the formation of active chromatin to induce gene expression profiles for foregut development (Hsu et al., 2015). These results suggest that RNAPII recruitment mediated by SPL15 could contribute to the removal of the repressive histone mark. Furthermore, the looping detected by 3C experiments at the *FUL* promoter, which is dependent on SOC1 and SPL15, might also be involved in the removal of H3K27me3 by REF6.

Previous studies in *Arabis alpina* showed that vernalization results in the upregulation of *SOC1* in both juvenile and adult plants, but fails to promote flowering in juvenile plants (Wang et al., 2011b). Thus SOC1 is insufficient to promote flowering in this relative species of *A. thaliana*, and further supports the idea that functional cooperation between SOC1 and miR156-targeted SPLs might be conserved for floral regulation in related species. It will now be important to address the precise roles of *SPL15* and its targets in the meristem in controlling floral transition,

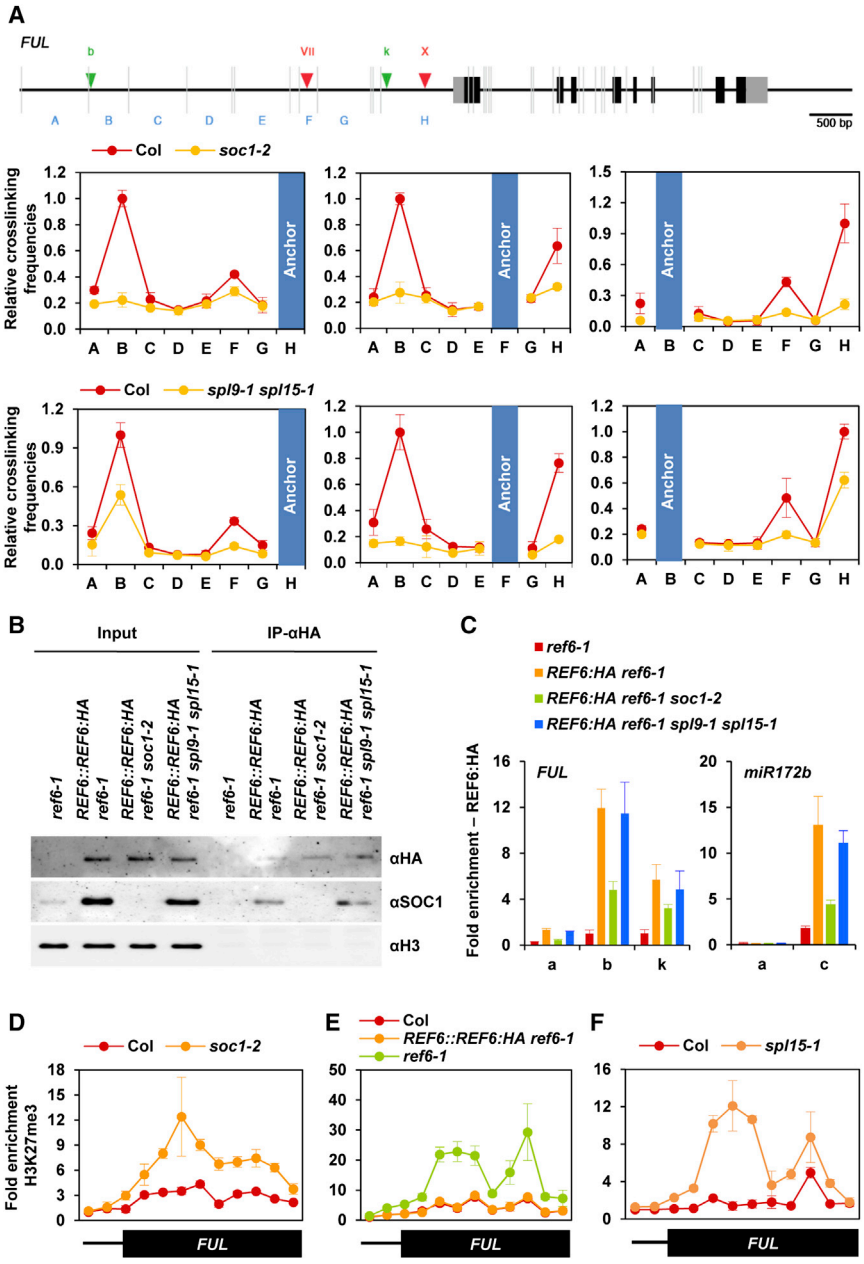

Figure 6. Roles of SOC1 in Removal of H3K27me3

(A) 3C analysis of the DNA loop formation at *FUL* locus. Top: a high-resolution digestion map of the *FUL* genomic region by the restriction enzyme *Sau*3AI is presented. Vertical gray lines indicate *Sau*3AI recognition sites. SOC1 and SPL15 binding sites are indicated by green and red arrowheads, respectively. The analyzed chromatin segments are indicated in blue below the corresponding regions. The regions bound by the anchored primers are marked with blue boxes in each graph portraying the results. The relative crosslinking frequency was corrected for ligation and PCR amplification efficiency using plasmid DNA containing a whole genomic region of *FUL* as a control template after digestion and ligation. The highest value is set to 1.0. Error bars indicate the SD of three independent biological replicates.

(B) In vivo coIP analysis of the protein interaction of SOC1 and REF6 in *35S::SOC1:MYC REF6::REF6:HA* plants.

(C) ChIP-qPCR analysis of REF6 enrichment at *FUL* and *miR172b* genomic loci. Positions of the analyzed amplicons correspond to those in Figure S5B.

(D–F) ChIP-qPCR analysis of H3K27me3 profiles at the transcribed region of *FUL* in *soc1* (D), *ref6* (E), and *spl* (F) mutant backgrounds.

See also Figure S6.

commitment to flowering, and behavior of the inflorescence meristem.

EXPERIMENTAL PROCEDURES

Plant Materials and Growth Conditions

For all studies, *A. thaliana* (L.) ecotype Columbia (Col-0) was used as wild-type, and all mutants and transgenic plants were in Col-0 background. Plants were grown on soil under controlled conditions of LDs (16 hr light/8 hr dark) and SDs (8 hr light/16 hr dark) at 20°C. The level of photosynthetic active radiation was 150 μmol/m^{-2} s^{-1} under both conditions. For GA treatment analyses, GA_4 stock (Sigma) was prepared in 100% ethanol with a final concentration of 1 mM. GA treatments were performed by spraying (twice per week) with either a GA solution (GA_4 10 μM, Silwet 77 0.02%) or a mock solution (ethanol 1%, Silwet 77 0.02%).

RNA Extraction and qRT-PCR

Total RNA was isolated from plant tissues using an RNAeasy extraction kit (Qiagen). 1–2 μg of total RNA was used for reverse transcription (Superscript III, Invitrogen) and transcript levels were quantified by qPCR in a LightCycler 480 instrument (Roche) using the *UBC21/PEX4* gene (AT5G25760) as a standard. The sequences of the primers used in the qRT-PCR analyses are listed in Table S2.

In Situ Hybridization and Confocal Microscopic Analyses

In situ hybridization was performed according to the method already described (Torti et al., 2012). The sequences of primers to generate the probes of *SPL15* mRNA are listed in Table S2. The probes used in the previous study were used for *FUL* and *SOC1* mRNA analyses. For the detection of mature miR172, the synthetic probe (osa-miR172a, Exiqon) was used. For V9A:SPL15 visualization in shoot meristems, a method described previously was used (Andres et al., 2015).

Plasmid Construction and Plant Transformation

Full-length *SPL15* genomic region was cloned by PCR and used to generate *V9A:SPL15* and *V9A:rSPL15*. To introduce the mutation at miR156 target site and the *Venus9Ala* coding sequences, we employed the polymerase incomplete primer extension cloning method (Klock and Lesley, 2009). The plasmids were then introduced into *Agrobacterium* to transform Col plants by floral dip (Clough and Bent, 1998). The sequences of primers used in the construction are listed in Table S2.

Yeast Two-Hybrid and Three-Hybrid Analyses

Yeast two-hybrid analysis using the Proquest Two-Hybrid system (Invitrogen) was performed according to the manufacturer's protocol with minor

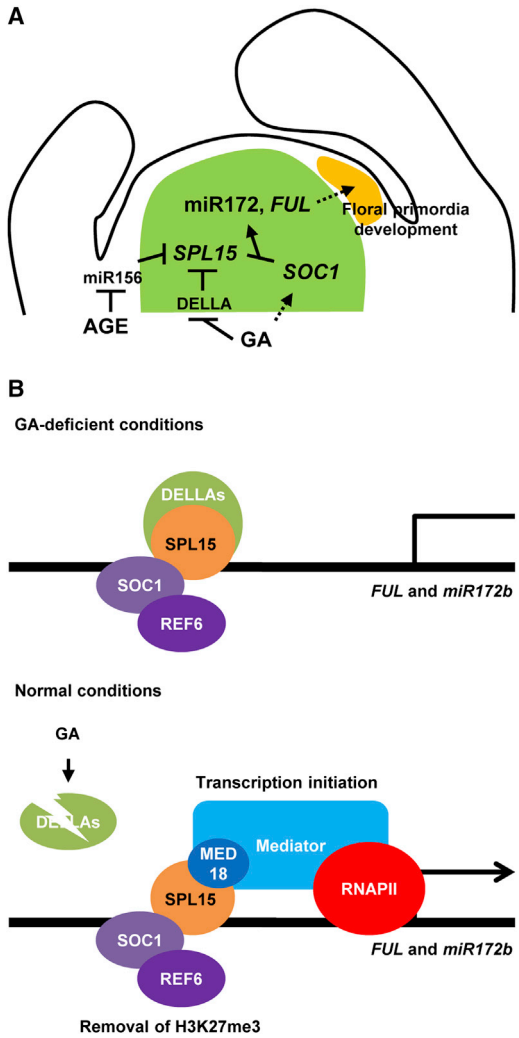

Figure 7. Roles of *SPL15* in Flowering of *Arabidopsis*

(A) Schematic illustration of the basal floral promotion pathway active under short-day conditions in the SAM of *A. thaliana*. Dashed lines indicate the genetic pathways with molecular mechanisms to be characterized.

(B) Schematic picture of the proposed cooperation between SPL15 and SOC1 to activate transcription of downstream target genes.

modifications. The constructed recombinant clones were introduced into MV203 yeast cells following the manufacturer's protocol. For yeast three-hybrid studies SPL15, RGA, and MED18 were cloned into pBridge and pGAD-T7 vectors (Clontech), respectively. Transformed yeast colonies were examined for growth on -Ade/-His/-Leu/-Trp quadruple dropout medium, which contains 3-AT to determine interactions. At least three independent tests were performed for each yeast strain.

ChIP-qPCR, In Vivo CoIP, and 3C Assays

ChIP analysis was performed as described previously with minor modifications (Mateos et al., 2015). The chromatin was extracted from LD-grown 14-day-old seedlings. Real-time qPCR was performed, and the relative enrichment of the IP/Input at each genomic region was normalized to that of the reference locus, *ACT8*. The amino acid sequences of epitopes for the generation of SPL15 and SOC1 antibodies and the list of antibodies used in the analyses are presented in Table S2. The in vivo coIP was performed as described previously with minor modifications (Willige et al., 2007). Roughly 40 apices of 14-day-old LD-grown seedlings were harvested and protein extracts were further nuclear enriched as described previously (Mateos et al., 2015). 3C analysis was performed as described previously with minor modifications (Hagege et al., 2007; Liu et al., 2014). The sequences of the primers used in ChIP-qPCR and 3C-qPCR are listed in Table S2.

SUPPLEMENTAL INFORMATION

Supplemental Information includes six figures and two tables and can be found with this article online at http://dx.doi.org/10.1016/j.devcel.2016.04.001.

AUTHOR CONTRIBUTIONS

G.C. and Y.H. initiated the project and coordinated the activities of co-authors; Y.H. and R.R. designed and carried out the genetic, molecular, and biochemical studies; and R.R. contributed the majority of biochemical results. Y.H., C.V., and R.M.-G. performed cellular and imaging studies. Y.H., R.R., and R.M.-G. generated transgenic *Arabidopsis* plants. R.R. and A.P. conducted the yeast two-hybrid assay for SPL15-RGA interaction. G.C. and Y.H. wrote the manuscript, with contributions from R.R.

ACKNOWLEDGMENTS

We thank Peter Huijser, Detlef Weigel, Hao Yu, and Xiaofeng Cao for generously providing materials, as well as Miltos Tsiantis and Franziska Turck for comments on the manuscript. The laboratory of G.C. is supported by the Cluster of Excellence in Plant Sciences (CEPLAS), the DFG through SPP1530, the ERC through HyLife, and a core grant from the Max Planck Society. Y.H. is supported by the Basic Science Research Program through the National Research Foundation of Korea (NRF) and the Ministry of Education (NRF-2011-357-C00134).

Received: December 17, 2015
Revised: March 16, 2016
Accepted: April 1, 2016
Published: April 28, 2016

REFERENCES

Abe, M., Kobayashi, Y., Yamamoto, S., Daimon, Y., Yamaguchi, A., Ikeda, Y., Ichinoki, H., Notaguchi, M., Goto, K., and Araki, T. (2005). FD, a bZIP protein mediating signals from the floral pathway integrator FT at the shoot apex. Science *309*, 1052–1056.

Adelman, K., and Lis, J.T. (2012). Promoter-proximal pausing of RNA polymerase II: emerging roles in metazoans. Nat. Rev. Genet. *13*, 720–731.

Andres, F., and Coupland, G. (2012). The genetic basis of flowering responses to seasonal cues. Nat. Rev. Genet. *13*, 627–639.

Andres, F., Romera-Branchat, M., Martinez-Gallegos, R., Patel, V., Schneeberger, K., Jang, S., Altmuller, J., Nurnberg, P., and Coupland, G. (2015). Floral induction in *Arabidopsis thaliana* by FLOWERING LOCUS T requires direct repression of BLADE-ON-PETIOLE genes by homeodomain protein PENNYWISE. Plant Physiol. *169*, 2187–2199.

Aukerman, M.J., and Sakai, H. (2003). Regulation of flowering time and floral organ identity by a MicroRNA and its APETALA2-like target genes. Plant Cell *15*, 2730–2741.

Bergonzi, S., Albani, M.C., Ver Loren van Themaat, E., Nordstrom, K.J., Wang, R., Schneeberger, K., Moerland, P.D., and Coupland, G. (2013). Mechanisms of age-dependent response to winter temperature in perennial flowering of *Arabis alpina*. Science *340*, 1094–1097.

Bonawitz, N.D., Kim, J.I., Tobimatsu, Y., Ciesielski, P.N., Anderson, N.A., Ximenes, E., Maeda, J., Ralph, J., Donohoe, B.S., Ladisch, M., et al. (2014). Disruption of Mediator rescues the stunted growth of a lignin-deficient *Arabidopsis* mutant. Nature *509*, 376–380.

Borner, R., Kampmann, G., Chandler, J., Gleissner, R., Wisman, E., Apel, K., and Melzer, S. (2000). A MADS domain gene involved in the transition to flowering in *Arabidopsis*. Plant J. *24*, 591–599.

Bowers, J.E., Chapman, B.A., Rong, J., and Paterson, A.H. (2003). Unravelling angiosperm genome evolution by phylogenetic analysis of chromosomal duplication events. Nature *422*, 433–438.

Chen, X. (2004). A microRNA as a translational repressor of APETALA2 in *Arabidopsis* flower development. Science *303*, 2022–2025.

Chuck, G., Cigan, A.M., Saeteurn, K., and Hake, S. (2007). The heterochronic maize mutant Corngrass1 results from overexpression of a tandem microRNA. Nat. Genet. *39*, 544–549.

Clough, S.J., and Bent, A.F. (1998). Floral dip: a simplified method for Agrobacterium-mediated transformation of *Arabidopsis thaliana*. Plant J. *16*, 735–743.

Eriksson, S., Bohlenius, H., Moritz, T., and Nilsson, O. (2006). GA4 is the active gibberellin in the regulation of LEAFY transcription and *Arabidopsis* floral initiation. Plant Cell *18*, 2172–2181.

Ferrandiz, C., Gu, Q., Martienssen, R., and Yanofsky, M.F. (2000). Redundant regulation of meristem identity and plant architecture by FRUITFULL, APETALA1 and CAULIFLOWER. Development *127*, 725–734.

Fu, X., Richards, D.E., Fleck, B., Xie, D., Burton, N., and Harberd, N.P. (2004). The *Arabidopsis* mutant sleepy1gar2-1 protein promotes plant growth by increasing the affinity of the SCFSLY1 E3 ubiquitin ligase for DELLA protein substrates. Plant Cell *16*, 1406–1418.

Galvao, V.C., Horrer, D., Kuttner, F., and Schmid, M. (2012). Spatial control of flowering by DELLA proteins in *Arabidopsis thaliana*. Development *139*, 4072–4082.

Hagege, H., Klous, P., Braem, C., Splinter, E., Dekker, J., Cathala, G., de Laat, W., and Forne, T. (2007). Quantitative analysis of chromosome conformation capture assays (3C-qPCR). Nat. Protoc. *2*, 1722–1733.

Hemsley, P.A., Hurst, C.H., Kaliyadasa, E., Lamb, R., Knight, M.R., De Cothi, E.A., Steele, J.F., and Knight, H. (2014). The *Arabidopsis* mediator complex subunits MED16, MED14, and MED2 regulate mediator and RNA polymerase II recruitment to CBF-responsive cold-regulated genes. Plant Cell *26*, 465–484.

Hsu, H.T., Chen, H.M., Yang, Z., Wang, J., Lee, N.K., Burger, A., Zaret, K., Liu, T., Levine, E., and Mango, S.E. (2015). TRANSCRIPTION. Recruitment of RNA polymerase II by the pioneer transcription factor PHA-4. Science *348*, 1372–1376.

Huijser, P., and Schmid, M. (2011). The control of developmental phase transitions in plants. Development *138*, 4117–4129.

Immink, R.G., Pose, D., Ferrario, S., Ott, F., Kaufmann, K., Valentim, F.L., de Folter, S., van der Wal, F., van Dijk, A.D., Schmid, M., et al. (2012). Characterization of SOC1's central role in flowering by the identification of its upstream and downstream regulators. Plant Physiol. *160*, 433–449.

Jung, J.H., Ju, Y., Seo, P.J., Lee, J.H., and Park, C.M. (2012). The SOC1-SPL module integrates photoperiod and gibberellic acid signals to control flowering time in *Arabidopsis*. Plant J. *69*, 577–588.

Klock, H.E., and Lesley, S.A. (2009). The Polymerase Incomplete Primer Extension (PIPE) method applied to high-throughput cloning and site-directed mutagenesis. Methods Mol. Biol. *498*, 91–103.

Lee, J., and Lee, I. (2010). Regulation and function of SOC1, a flowering pathway integrator. J. Exp. Bot. *61*, 2247–2254.

Lee, H., Suh, S.S., Park, E., Cho, E., Ahn, J.H., Kim, S.G., Lee, J.S., Kwon, Y.M., and Lee, I. (2000). The AGAMOUS-LIKE 20 MADS domain protein integrates floral inductive pathways in *Arabidopsis*. Genes Dev. *14*, 2366–2376.

Liu, L.Y., Adrian, J., Pankin, A., Hu, J.Y., Dong, X., von Korff, M., and Turck, F. (2014). Induced and natural variation of promoter length modulates the photoperiodic response of FLOWERING LOCUS T. Nat Commun. *5*, 4558.

Lu, F., Cui, X., Zhang, S., Jenuwein, T., and Cao, X. (2011). *Arabidopsis* REF6 is a histone H3 lysine 27 demethylase. Nat. Genet. *43*, 715–719.

Malik, S., and Roeder, R.G. (2010). The metazoan Mediator co-activator complex as an integrative hub for transcriptional regulation. Nat. Rev. Genet. *11*, 761–772.

Mateos, J.L., Madrigal, P., Tsuda, K., Rawat, V., Richter, R., Romera-Branchat, M., Fornara, F., Schneeberger, K., Krajewski, P., and Coupland, G. (2015). Combinatorial activities of SHORT VEGETATIVE PHASE and FLOWERING LOCUS C define distinct modes of flowering regulation in *Arabidopsis*. Genome Biol. *16*, 31.

Mathieu, J., Yant, L.J., Murdter, F., Kuttner, F., and Schmid, M. (2009). Repression of flowering by the miR172 target SMZ. PLoS Biol. *7*, e1000148.

Melzer, S., Lens, F., Gennen, J., Vanneste, S., Rohde, A., and Beeckman, T. (2008). Flowering-time genes modulate meristem determinacy and growth form in *Arabidopsis thaliana*. Nat. Genet. *40*, 1489–1492.

Moon, J., Suh, S.S., Lee, H., Choi, K.R., Hong, C.B., Paek, N.C., Kim, S.G., and Lee, I. (2003). The SOC1 MADS-box gene integrates vernalization and gibberellin signals for flowering in *Arabidopsis*. Plant J. *35*, 613–623.

Murase, K., Hirano, Y., Sun, T.P., and Hakoshima, T. (2008). Gibberellin-induced DELLA recognition by the gibberellin receptor GID1. Nature *456*, 459–463.

Noh, B., Lee, S.H., Kim, H.J., Yi, G., Shin, E.A., Lee, M., Jung, K.J., Doyle, M.R., Amasino, R.M., and Noh, Y.S. (2004). Divergent roles of a pair of homologous jumonji/zinc-finger-class transcription factor proteins in the regulation of *Arabidopsis* flowering time. Plant Cell *16*, 2601–2613.

Onouchi, H., Igeno, M.I., Perilleux, C., Graves, K., and Coupland, G. (2000). Mutagenesis of plants overexpressing CONSTANS demonstrates novel interactions among *Arabidopsis* flowering-time genes. Plant Cell *12*, 885–900.

Porri, A., Torti, S., Romera-Branchat, M., and Coupland, G. (2012). Spatially distinct regulatory roles for gibberellins in the promotion of flowering of *Arabidopsis* under long photoperiods. Development *139*, 2198–2209.

Rhoades, M.W., Reinhart, B.J., Lim, L.P., Burge, C.B., Bartel, B., and Bartel, D.P. (2002). Prediction of plant microRNA targets. Cell *110*, 513–520.

Samach, A., Onouchi, H., Gold, S.E., Ditta, G.S., Schwarz-Sommer, Z., Yanofsky, M.F., and Coupland, G. (2000). Distinct roles of CONSTANS target genes in reproductive development of *Arabidopsis*. Science *288*, 1613–1616.

Schmid, M., Uhlenhaut, N.H., Godard, F., Demar, M., Bressan, R., Weigel, D., and Lohmann, J.U. (2003). Dissection of floral induction pathways using global expression analysis. Development *130*, 6001–6012.

Schwab, R., Palatnik, J.F., Riester, M., Schommer, C., Schmid, M., and Weigel, D. (2005). Specific effects of microRNAs on the plant transcriptome. Dev. Cell *8*, 517–527.

Schwarz, S., Grande, A.V., Bujdoso, N., Saedler, H., and Huijser, P. (2008). The microRNA regulated SBP-box genes SPL9 and SPL15 control shoot maturation in *Arabidopsis*. Plant Mol. Biol. *67*, 183–195.

Silverstone, A.L., Jung, H.S., Dill, A., Kawaide, H., Kamiya, Y., and Sun, T.P. (2001). Repressing a repressor: gibberellin-induced rapid reduction of the RGA protein in *Arabidopsis*. Plant Cell *13*, 1555–1565.

Smaczniak, C., Immink, R.G., Muino, J.M., Blanvillain, R., Busscher, M., Busscher-Lange, J., Dinh, Q.D., Liu, S., Westphal, A.H., Boeren, S., et al. (2012). Characterization of MADS-domain transcription factor complexes in *Arabidopsis* flower development. Proc. Natl. Acad. Sci. USA *109*, 1560–1565.

Tao, Z., Shen, L., Liu, C., Liu, L., Yan, Y., and Yu, H. (2012). Genome-wide identification of SOC1 and SVP targets during the floral transition in *Arabidopsis*. Plant J. *70*, 549–561.

Torti, S., Fornara, F., Vincent, C., Andres, F., Nordstrom, K., Gobel, U., Knoll, D., Schoof, H., and Coupland, G. (2012). Analysis of the *Arabidopsis* shoot meristem transcriptome during floral transition identifies distinct regulatory patterns and a leucine-rich repeat protein that promotes flowering. Plant Cell *24*, 444–462.

Wang, J.W., Czech, B., and Weigel, D. (2009). miR156-regulated SPL transcription factors define an endogenous flowering pathway in *Arabidopsis thaliana*. Cell *138*, 738–749.

Wang, J.W., Park, M.Y., Wang, L.J., Koo, Y., Chen, X.Y., Weigel, D., and Poethig, R.S. (2011a). miRNA control of vegetative phase change in trees. PLoS Genet. *7*, e1002012.

Wang, R., Albani, M.C., Vincent, C., Bergonzi, S., Luan, M., Bai, Y., Kiefer, C., Castillo, R., and Coupland, G. (2011b). Aa TFL1 confers an age-dependent response to vernalization in perennial *Arabis alpina*. Plant Cell *23*, 1307–1321.

Wigge, P.A., Kim, M.C., Jaeger, K.E., Busch, W., Schmid, M., Lohmann, J.U., and Weigel, D. (2005). Integration of spatial and temporal information during floral induction in *Arabidopsis*. Science *309*, 1056–1059.

Willige, B.C., Ghosh, S., Nill, C., Zourelidou, M., Dohmann, E.M., Maier, A., and Schwechheimer, C. (2007). The DELLA domain of GA INSENSITIVE mediates the interaction with the GA INSENSITIVE DWARF1A gibberellin receptor of *Arabidopsis*. Plant Cell *19*, 1209–1220.

Wilson, R.N., Heckman, J.W., and Somerville, C.R. (1992). Gibberellin is required for flowering in *Arabidopsis thaliana* under short days. Plant Physiol. *100*, 403–408.

Wu, G., and Poethig, R.S. (2006). Temporal regulation of shoot development in *Arabidopsis thaliana* by miR156 and its target SPL3. Development *133*, 3539–3547.

Wu, G., Park, M.Y., Conway, S.R., Wang, J.W., Weigel, D., and Poethig, R.S. (2009). The sequential action of miR156 and miR172 regulates developmental timing in *Arabidopsis*. Cell *138*, 750–759.

Xu, M.L., Hu, T.Q., Smith, M.R., and Poethig, R.S. (2016). Epigenetic regulation of vegetative phase change in *Arabidopsis*. Plant Cell *28*, 28–41.

Yamaguchi, A., Wu, M.F., Yang, L., Wu, G., Poethig, R.S., and Wagner, D. (2009). The microRNA-regulated SBP-Box transcription factor SPL3 is a direct upstream activator of LEAFY, FRUITFULL, and APETALA1. Dev. Cell *17*, 268–278.

Yamaguchi, N., Winter, C.M., Wu, M.F., Kanno, Y., Yamaguchi, A., Seo, M., and Wagner, D. (2014). Gibberellin acts positively then negatively to control onset of flower formation in *Arabidopsis*. Science *344*, 638–641.

Yant, L., Mathieu, J., Dinh, T.T., Ott, F., Lanz, C., Wollmann, H., Chen, X., and Schmid, M. (2010). Orchestration of the floral transition and floral development in *Arabidopsis* by the bifunctional transcription factor APETALA2. Plant Cell *22*, 2156–2170.

Yu, S., Galvao, V.C., Zhang, Y.C., Horrer, D., Zhang, T.Q., Hao, Y.H., Feng, Y.Q., Wang, S., Schmid, M., and Wang, J.W. (2012). Gibberellin regulates the *Arabidopsis* floral transition through miR156-targeted SQUAMOSA promoter binding-like transcription factors. Plant Cell *24*, 3320–3332.

Zhang, F., Yao, J., Ke, J., Zhang, L., Lam, V.Q., Xin, X.F., Zhou, X.E., Chen, J., Brunzelle, J., Griffin, P.R., et al. (2015). Structural basis of JAZ repression of MYC transcription factors in jasmonate signalling. Nature *525*, 269–273.

Zheng, Z., Guan, H., Leal, F., Grey, P.H., and Oppenheimer, D.G. (2013). Mediator subunit18 controls flowering time and floral organ identity in *Arabidopsis*. PLoS One *8*, e53924.

Zhou, C.M., Zhang, T.Q., Wang, X., Yu, S., Lian, H., Tang, H., Feng, Z.Y., Zozomova-Lihova, J., and Wang, J.W. (2013). Molecular basis of age-dependent vernalization in *Cardamine flexuosa*. Science *340*, 1097–1100.

Developmental Cell, Volume *37*

Supplemental Information

Multi-layered Regulation of SPL15 and Cooperation with SOC1 Integrate Endogenous Flowering Pathways at the *Arabidopsis* Shoot Meristem

Youbong Hyun, René Richter, Coral Vincent, Rafael Martinez-Gallegos, Aimone Porri, and George Coupland

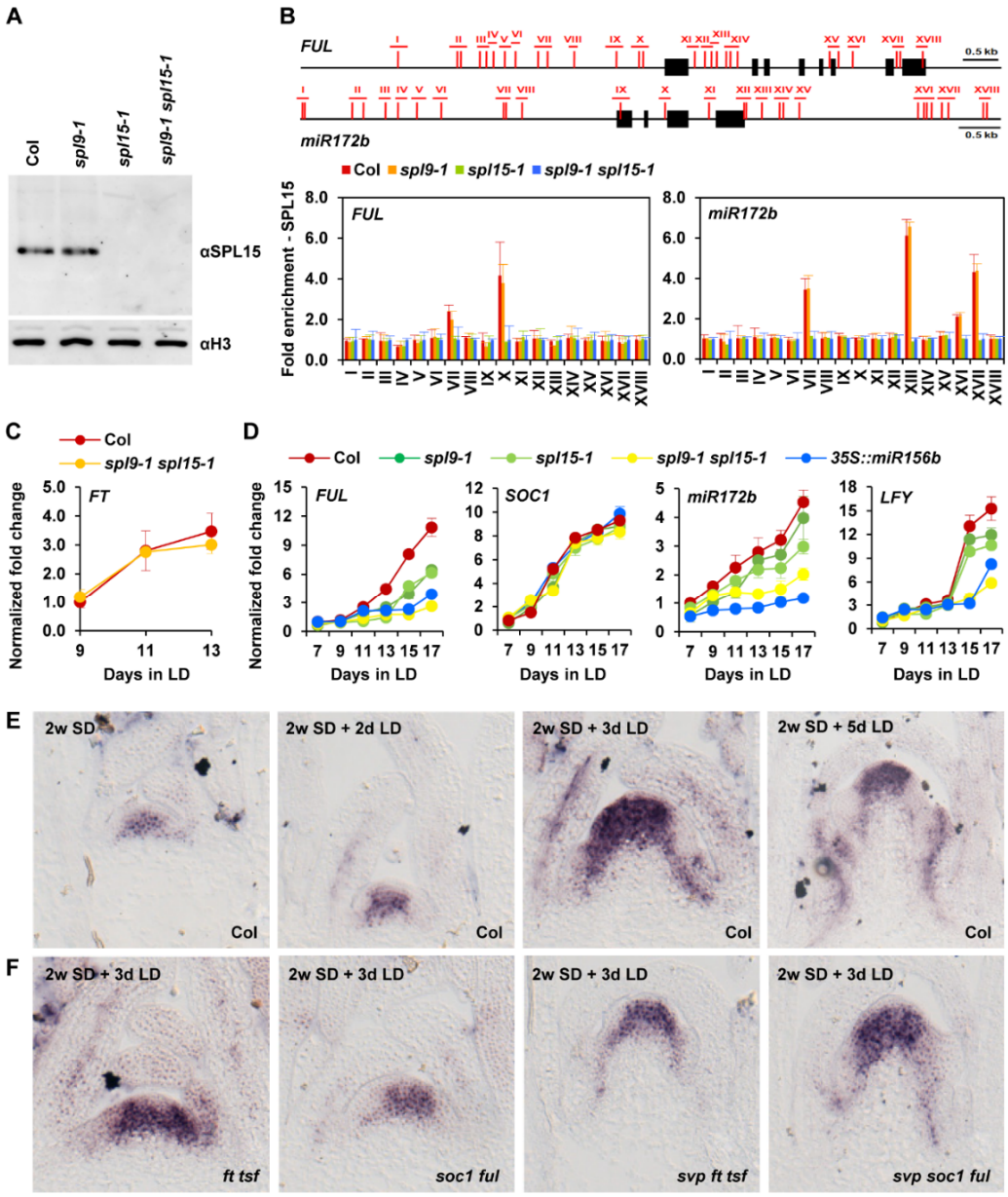

Figure S1, Related to Figure 1. Roles of *SPL15* in Flowering

(A) Result of Western blot analysis performed with antibodies for SPL15. To examine specificity of the antibodies, loss of function mutants of *SPL15* were included in the analysis. Total protein was extracted from apical samples and the nuclear proteins were further enriched. The same amount of total proteins were loaded on the gels. (B) ChIP-qPCR analysis of SPL15. Schematic structures of *FUL* and *miR172b* genomic regions are present at top. Exons and the predicted binding motifs of SPL transcription factors are presented by black boxes and vertical red bars, respectively. Horizontal red bars indicate amplicons in ChIP-qPCR analysis. Chromatin was extracted from 14 day-old LD-grown seedlings. Error bars indicate standard deviation among three independent biological replicates. (C) RT-qPCR analysis of *FT* mRNA levels during LD growth. Total RNA was extracted from whole seedlings at ZT16 in which *FT* shows a peak of expression. Error bars indicate standard deviation of three independent biological replicates. Transcript levels in 9 day-old Col plants are set to 1.0. (D) RT-qPCR analysis of *FUL*, *SOC1*, *miR172b* and *LFY* mRNA levels during LD growth. Total RNA was extracted from hand-dissected shoot apical samples. Error bars indicate standard deviation of three independent biological replicates. Transcript levels in 7 day-old Col plants are set to 1.0. (E) *In situ* hybridization analysis of *SPL15* mRNA during floral transition induced by SD to LD photoperiod shifts. (F) *In situ* hybridization analysis of *SPL15* mRNA in various flowering mutant backgrounds.

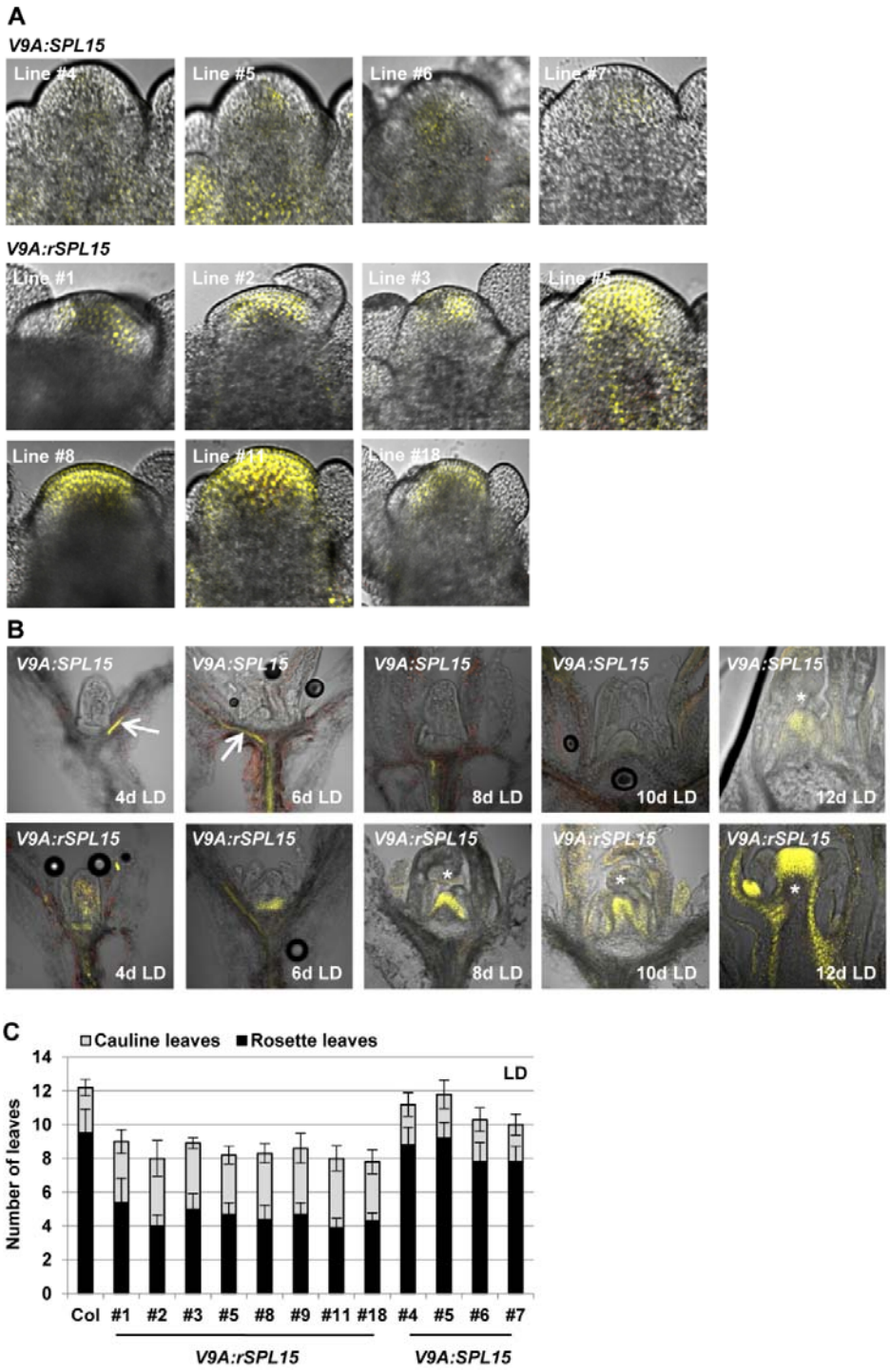

Figure S2, Related to Figure 3. *SPL15* Integrates Flowering Cues Derived from miR156
(A) Confocal microscopic analysis of fusion protein accumulation in independent *V9A:SPL15* and *V9A:rSPL15* transgenic lines at 7 days after transfer of 2 week-old SD grown plants to LDs. The analyses were performed with intact shoot apices without sectioning. (B) Confocal microscopic analysis of the fusion protein accumulation in *V9A:SPL15* and *V9A:rSPL15* during LD growth. Arrows and asterisks indicate autofluorescence from tracheary elements in vasculature and shoot apices undergoing bolting, respectively. (C) Flowering time of *V9A:SPL15* and *V9A:rSPL15* in LD conditions. Numbers of leaves were measured in T3 homozygous populations of the independent transgenic lines.

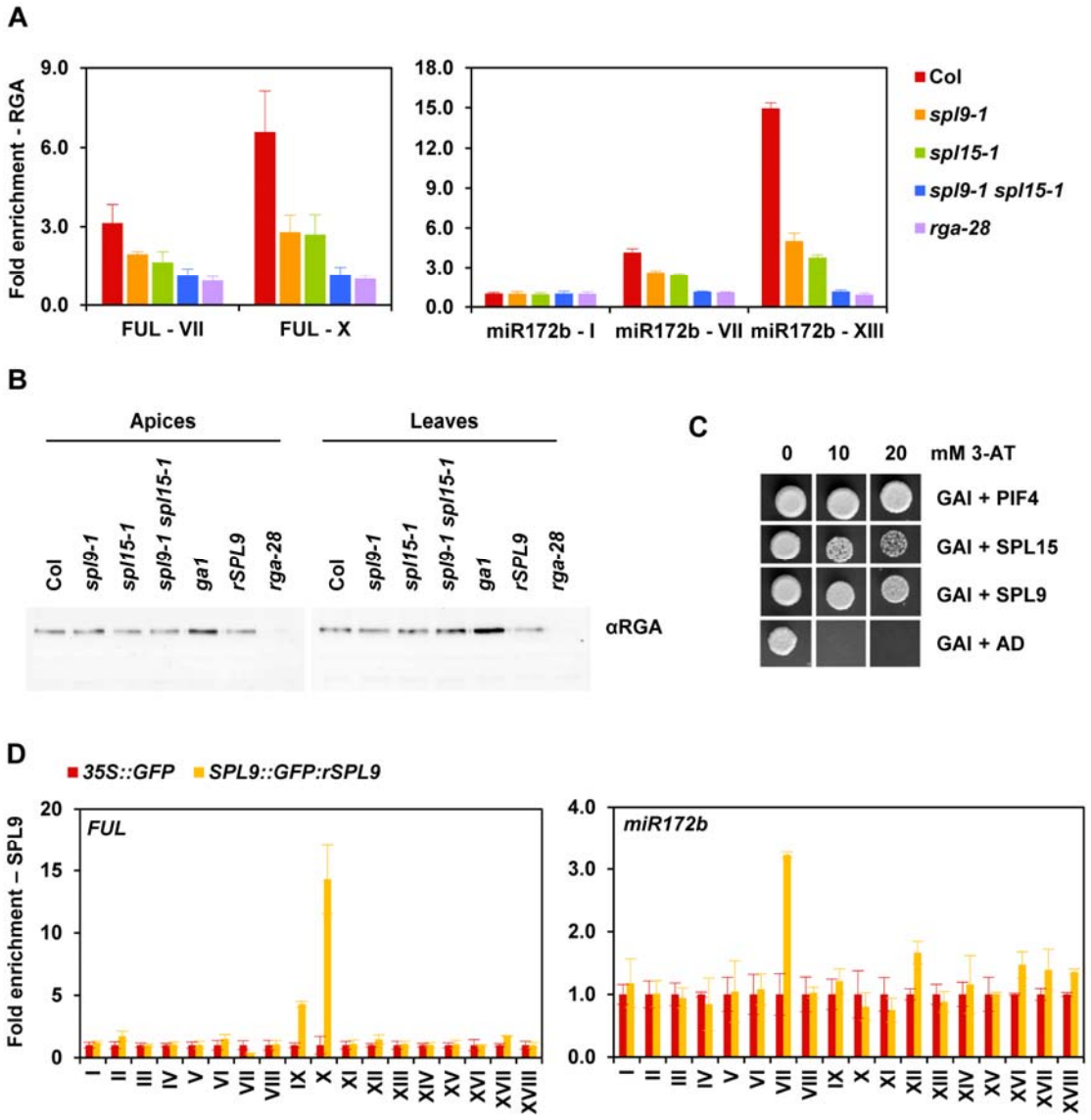

Figure S3, Related to Figure 3. Colocalization of RGA with SPL15 and SPL9 to the *FUL* and *miR172b* Genomic Loci

(A) ChIP-qPCR analysis of RGA enrichment in *spl* mutants. Chromatin was extracted from 14 day-old LD-grown seedlings. Error bars indicate standard deviation among three independent biological replicates. (B) Results of Western blot analysis performed with antibodies for RGA. To examine specificity of the antibodies, loss of function mutants of *RGA* were included in the analysis. Total protein was extracted from 14 day-old seedlings grown under LD conditions. The same amount of total proteins was loaded on the gels. (C) Yeast two-hybrid analysis of the interaction of GAI DELLA protein with SPL15 and SPL9. PIF4 was included in the analysis as a positive control for the interaction with GAI. (D) ChIP-qPCR analysis of SPL9 enrichment on *FUL* and *miR172b* loci. The analyzed amplicons are corresponding to those in Figure S1B. Chromatin was extracted from 14 day-old LD-grown seedlings. Error bars indicate standard deviation among three independent biological replicates.

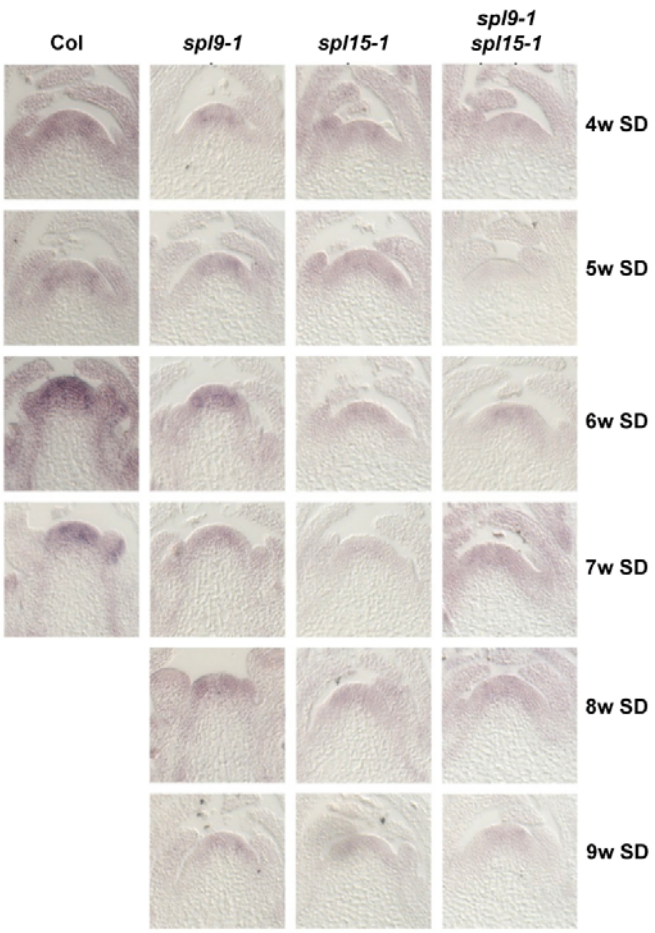

Figure S4, Related to Figure 4. Accumulation of *SOC1* mRNA in *spl* Mutants under SD Conditions
In situ hybridization analysis of *SOC1* mRNA expression in Col, *spl9*, *spl15* and *spl9 spl15* during SD growth.

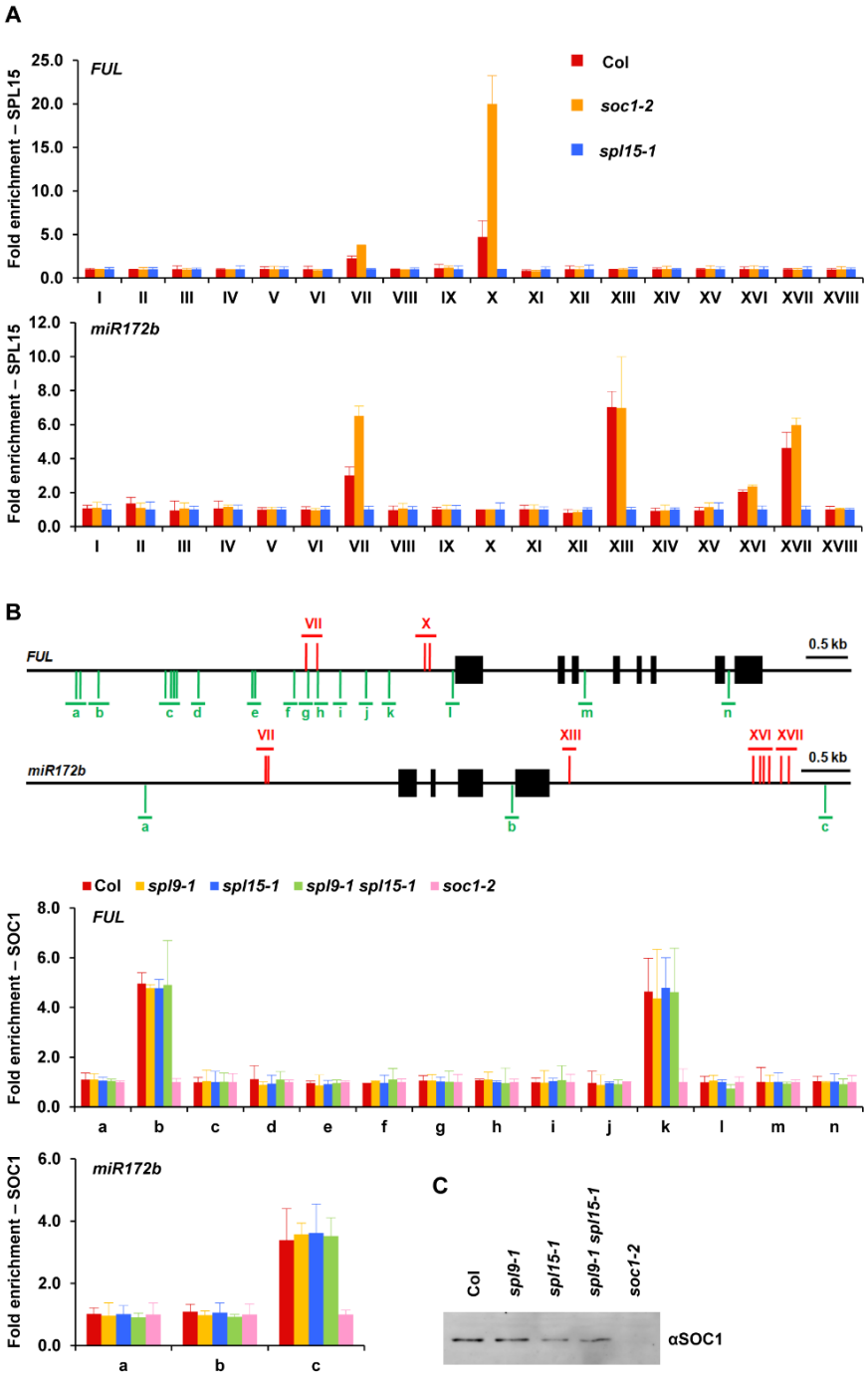

Figure S5, Related to Figure 4. Direct Targeting of SPL15 and SOC1 on *FUL* and *miR172b* Genomic Loci
(A) ChIP-qPCR analysis of SPL15 enrichment on *FUL* and *miR172b* genomic loci in *soc1* mutants. The analyzed amplicons are corresponding to those in Figure S1B. (B) ChIP-qPCR analysis of SOC1 enrichment profiles on *FUL* and *miR172b* genomic loci. Schematic structure of *FUL* and *miR172b* genomic region. Exons and the predicted binding motifs of SOC1 are presented by black boxes and vertical green bars, respectively. Horizontal green bars indicate amplicons in ChIP-qPCR analysis. The SPL15-enriched amplicons are also shown by red bars. Chromatin was extracted from 14 day-old LD-grown seedlings. Error bars indicate standard deviation among three independent biological replicates. (C) Western blot analysis performed with antibodies for SOC1. To examine specificity of the antibodies, loss of function mutants of *SOC1* were included in the analyses. The same amount of total proteins were loaded on the gels.

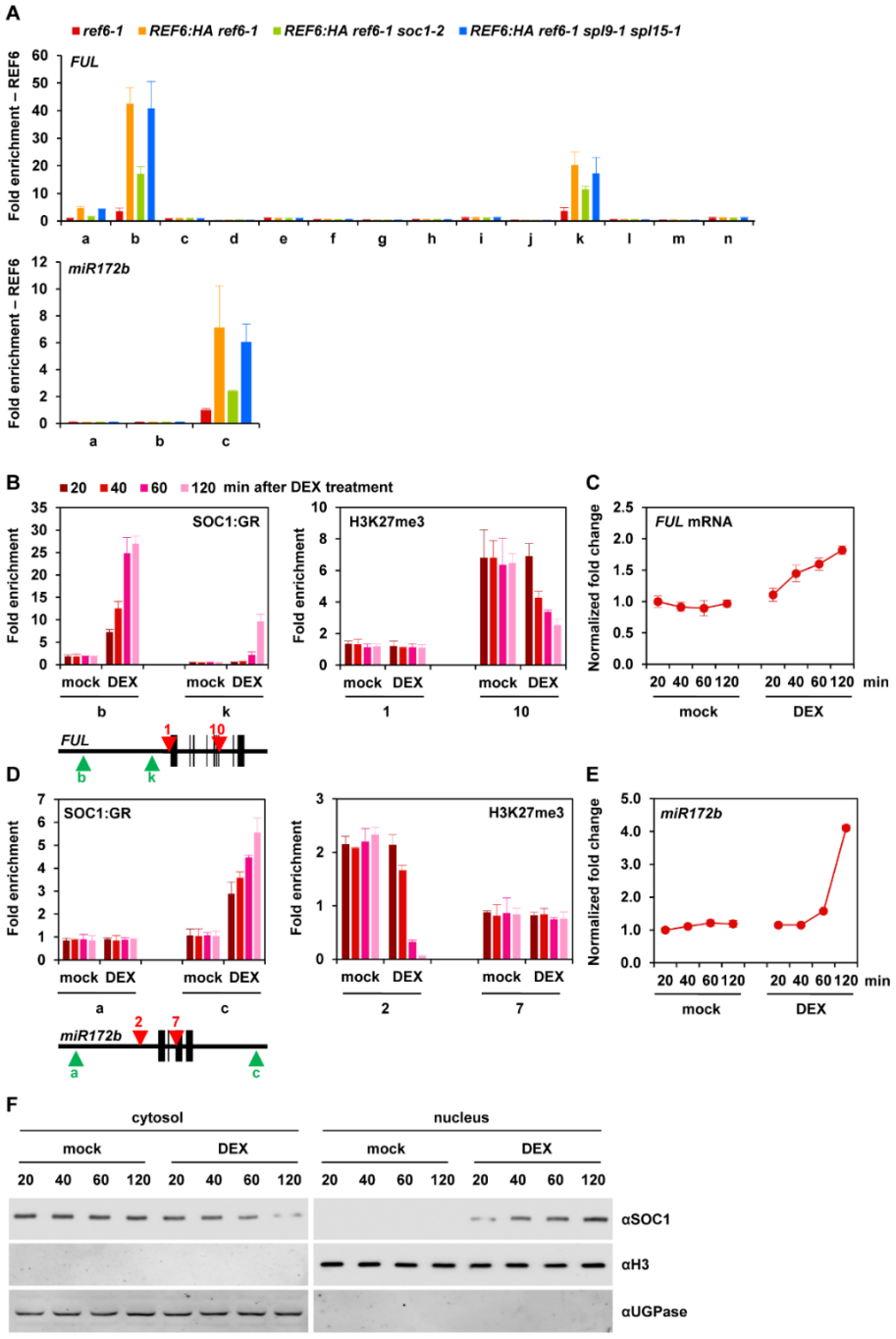

Figure S6, Related to Figure 6. SOC1-induced Removal of H3K27me3 and Transcriptional Activation
(A) ChIP-qPCR analysis of REF6:HA enrichment on *FUL* and *miR172b* genomic loci. The analyzed amplicons are corresponding to those in Figure S5B. Chromatin was extracted from 14 day-old LD-grown seedlings. Antibody for HA was used in the ChIP analyses. Error bars indicate standard deviation among three independent biological replicates. (B to E) SOC1-induced transcriptional activation of *FUL* and *miR172b*. ChIP-qPCR analysis of SOC1 and H3K27me3 enrichments on *FUL* (B) and *miR172b* (D) in *35S::SOC1:GR soc1-1* plants after DEX treatment. The corresponding positions of the analyzed amplicons are presented at bottom panel. RT-qPCR analysis of *FUL* mRNA (C) and *miR172b* (E) levels in *35S::SOC1:GR soc1-1* after DEX treatment. (F) Western blot analysis for kinetics of SOC1:GR nuclear translocation. UGPase and H3 present markers of the purified cytosolic and nuclear fractions, respectively.

Table S1, Related to Figure 1, 3 and 4. Flowering Time Analyses of *spl9*, *spl15* and Related Transgenic Plants

Conditions	Leaf numbers		Days	Numbers of analyzed plants
	Rosette	Cauline		
Experiment 1 (SD)				
Col-0	50.3 ± 4.3	8.0 ± 1.3	73.2 ± 8.6	24
spl9-1	51.3 ± 3.9	7.8 ± 1.8	75.3 ± 7.9	24
spl15-1	>80	n.a.*	133.6 ± 7.3	28
spl9-1 spl15-1	>80	n.a.*	141.3 ± 9.7	28
35S::miR156b	>80	n.a.*	148.7 ± 12.7	28
Experiment 2 (SD)				
Col-0	49.2 ± 3.7	6.2 ± 0.9	67.9 ± 7.3	28
spl9-2	51.1 ± 3.4	7.1 ± 1.4	68.6 ± 6.9	28
spl15-2	>80	n.a.*	130.6 ± 9.2	28
spl9-2 spl15-2	>80	n.a.*	135.9 ± 13.6	28
Experiment 3 (LD)				
Col-0	12.5 ± 1.9	2.4 ± 1.2	23.3 ± 1.8	24
spl9-1	14.0 ± 2.0	1.7 ± 1.2	24.3 ± 2.1	24
spl15-1	16.2 ± 2.2	3.1 ± 0.5	26.3 ± 2.3	22
spl9-1 spl15-1	19.2 ± 4.1	2.9 ± 1.2	28.5 ± 2.9	24
spl9-2	14.5 ± 3.1	2.3 ± 2.8	26.6 ± 3.3	24
spl15-2	16.3 ± 1.8	2.8 ± 1.7	25.5 ± 2.1	24
spl9-2 spl15-2	15.5 ± 3.1	2.7 ± 1.5	25.4 ± 2.9	23
35S::miR156b	22.2 ± 2.4	n.a.*	27.1 ± 2.2	24
Experiment 4				
(SD + Mock)				
Col-0	53.7 ± 3.1	8.7 ± 2.0	70.2 ± 4.9	24
spl9-1	55.0 ± 3.7	8.8 ± 1.9	73.0 ± 1.5	24
spl15-1	>80	n.a.*	124.7 ± 5.4	24
spl9-1 spl15-1	>80	n.a.*	129.8 ± 3.6	28
35S::miR156b	>80	n.a.*	138.8 ± 4.3	28
(SD + GA)				
Col-0	33.3 ± 2.7	12.5 ± 2.6	55.2 ± 3.3	28
spl9-1	34.4 ± 4.5	9.6 ± 1.7	56.6 ± 3.7	28
spl15-1	73.2 ± 3.1	10.2 ± 2.1	102.5 ± 6.1	24
spl9-1 spl15-1	>80	n.a.*	111.7 ± 6.3	28
35S::miR156b	>80	n.a.*	114.7 ± 6.0	28
Experiment 5 (SD)				
Col-0	52.8 ± 7.3	10.6 ± 2.3	n.a.*	28
V9A:rSPL15	16.0 ± 1.9	7.4 ± 2.6	n.a.*	24
V9A:rSPL15 KNAT1::GA2ox7	71.0 ± 6.3	0.0	n.a.*	28
KNAT1::GA2ox7	79.6 ± 5.8	0.0	n.a.*	26
Experiment 6 (SD)				
Col-0	57.1 ± 5.1	11.3 ± 2.5	n.a.*	24
V9A:rSPL15	20.2 ± 1.5	6.2 ± 1.1	n.a.*	24
V9A:rSPL15 soc1-2 ful-2	>80	n.a.*	n.a.*	24
soc1-2 ful-2	>80	n.a.*	n.a.*	24

*n.a., not analyzed

Table S2, Related to Experimental Procedures. List of Primers, Antibodies and Epitopes Used in the Study